Lorena Pardo
Jesús Ricote
Editors

SPRINGER SERIES IN MATERIALS SCIENCE 140

Multifunctional Polycrystalline Ferroelectric Materials

Processing and Properties

Springer

Springer Series in
MATERIALS SCIENCE 140

Springer Series in
MATERIALS SCIENCE

The Springer Series in Materials Science covers the complete spectrum of materials physics, including fundamental principles, physical properties, materials theory and design. Recognizing the increasing importance of materials science in future device technologies, the book titles in this series reflect the state-of-the-art in understanding and controlling the structure and properties of all important classes of materials.

For other titles published in this series, go to
www.springer.com/series/856

Lorena Pardo • Jesús Ricote

Multifunctional Polycrystalline Ferroelectric Materials

Processing and Properties

Springer

Piezo INSTITUTE
The European Institute of Piezoelectric Materials and Devices

Professor Dr. Lorena Pardo
Instituto de Ciencia de Materiales
de Madrid
Consejo Superior de Investigaciones
Científicas
(ICMM-CSIC)
Cantoblanco
28049 Madrid
España

Dr. Jesús Ricote
Instituto de Ciencia de Materiales
de Madrid
Consejo Superior de Investigaciones
Científicas
(ICMM-CSIC)
Cantoblanco
28049 Madrid
España

Published by Springer,
P.O. Box 17, 3300 AA Dordrecht, The Netherlands
In association with
Canopus Academic Publishing Limited,
15 Nelson Parade, Bedminster, Bristol, BS3 4HY, UK

www.springer.com and www.canopusbooks.com

Springer Series in Materials Science ISSN 0933-033X
ISBN 978-90-481-2874-7 e-ISBN 978-90-481-2875-4
Springer Dordrecht Heidelberg London New York

Library of Congress Control Number: 2009940448

Printed on acid-free paper

Springer is part of Springer Science+Business Media (www.springer.com)

Preface

Most of the recent efforts to produce books on ferroelectric materials have focused on issues such as the integration of ferroelectrics into different types of devices (Ferrolectric and Dynamic Random Access Memories; Piezoelectric Devices), mostly in thin film form, with intrusions into the realm of nanoscale phenomena. Although some attempts have been made to cover more fundamental topics, such as mechanical fatigue or phase transitions, which are essential to understand the performance of polycrystalline ferroelectrics in applications, an overview of the recent advances in processing and properties of both ferroelectric bulk ceramics and thin films is still lacking, despite its direct impact on the improvement or development of new applications. We think that this book can fill such gap. Here the reader will find in one book updated information on the preparation and properties of this technologically relevant range of materials – information that is currently scattered throughout a number of publications.

Basic concepts of polycrystalline ferroelectrics processing and properties are found, together with references to their multiple applications, in the introductory sections of the chapters. On the other hand, research topics that arose in the recent past and are nowadays the focus of intense activity are also addressed in this book. Such is the case for the environmentally friendly polycrystalline ferro-piezoelectric materials, seen from the point of view of elimination of hazardous components, such as the commonly used lead oxide, or the development of clean processing routes for lead-based ferroelectrics. The challenges in the processing and characterization of crystallographically oriented bulk ferroelectric ceramics and nanosized ferroelectrics are also analysed here. All chapters were written by leading authorities on the topics with reference to the basics and to recent advances.

C. Galassi (ISTEC, Faenza, Italy) has written *Advances in Processing of Bulk Ferroelectric Materials,* using both classical and non-conventional techniques. M. Kosec, D. Kuscer and J. Holc (Institute Jožef Stefan, Ljubljana, Slovenia) have written *Processing of Ferroelectric Ceramic Thick Films,* a topic at the first stage of the integration of ferroelectrics with other hybrid and microelectronic technolo-

gies. Following the integration steps that require even higher reduction of the dimensions of the ferroelectric material, some chapters are devoted to thin-film issues and nano-sized ferroelectrics. K. Kato (National Institute of Advanced Industrial Science and Technology (AIST), Nagoya, Japan) has written *Tailored Liquid Alkoxides for the Chemical Solution Processing of Pb-free Ferroelectric Thin Films*. M. L. Calzada (ICMM-CSIC, Madrid, Spain) has written *Ferroelectrics onto Substrates Prepared by Chemical Solution Deposition: From the Thin Film to the Self-Assembled Nano-sized Structures* and I. Bretos and M. L. Calzada (ICMM-CSIC. Madrid, Spain) have written *Approaches Towards the Minimisation of Toxicty in Chemical Solution Deposition Processes of Lead-Based Ferroelectric Thin Films.*

Ferroelectricity and crystal structure are closely related, and the detailed analysis of this requires the use of singular and advanced techniques. L. E. Fuentes-Cobas (Centro de Investigación de Materiales Avanzados, Chihuahua, México) has written about *Synchrotron Radiation Diffraction and Scattering in Ferroelectrics*; M. E. Montero Cabrera (Centro de Investigación de Materiales Avanzados. Chihuahua, Mexico) – *X-Ray Absorption Fine Structure Applied to Ferroelectrics*; D. Chateigner (CRISMAT-ENSICAEN, Caen, France) and J. Ricote (ICMM-CSIC, Madrid, Spain) – *Quantitative Texture Analysis of Polycrystalline Ferroelectrics; and* V. V. Svartsman (Duisburg-Essen University. Duisburg, Germany); and A. L. Kholkin (Aveiro University. Aveiro, Portugal) –*Nanoscale Investigation of Polycrystalline Ferroelectric Materials Via Piezoresponse Force Microscopy.*

Frequently ferro-piezoelectric ceramic materials in devices are subjected to high mechanical loads and must present a high resistance to fatigue under electromechanical vibrations. D. Lupascu, J. Schröder (University of. Duisburg-Essen, Essen, Germany), C. Lynch (UCLA, Los Angeles, USA), W. Kreher (University of Dresden, Dresden, Germany) and I. Westram (Darmstadt University of Technology, Darmstadt, Germany) have written about *Mechanical Properties of Ferro-Piezoceramics*. C. Chima-Okereke, W. L. Roberts, A. J. Bushby and M. J. Reece (Queen Mary College, University of London, UK) have written about *The Elastic Properties of Ferroelectric Thin Films Using Nanoindentation.*

A glimpse of the multifunctionality of ferro-piezoelectric ceramics, also mentioned in other chapters, is provided by R. Jiménez and B. Jiménez (ICMM-CSIC, Madrid, Spain), writing on *Pyroelectricity in Polycrystalline Ferroelectrics*. Special attention was given to issues related to the piezoelectric properties of polycrystalline ferroelectrics which are far from being fully explored, and nowadays face important challenges. L. Pardo (ICMM-CSIC, Madrid, Spain) and K. Brebøl (Limiel ApS, Langebæk, Denmark) cover *Properties of Ferro-Piezoelectric Ceramic Materials in the Linear Range: Determination from Impedance Measurements at Resonance* and J. Erhart (Technical University of Liberec, Liberec, Czech Republic) describes *Domain Engineered Piezoelectric Resonators.* A. Albareda and R. Pérez (Politechnic University of Catalonia, Barcelona, Spain) have written about *Non-linear Behaviour of Piezoelectric Ceramics*. Finally, also as a glimpse into the many possible applications of polycrystalline ferroelectrics, in particular in the field of ultrasonic transducers,

Y. Gómez-Ullate Ricón and F. Montero de Espinosa Freijo (Acoustics Institute, CSIC, Madrid, Spain) have written *Piezoelectric Transducers for Structural Health Monitoring: Modelling and Imaging.*

This book offers interesting content for the beginner from academia or industry who is curious about the possibilities of polycrystalline ferroelectric materials; they will find here a wide range of information. But, also, researchers involved in the study of ferroelectric materials or end-users of ferro-piezoelectric ceramics will find some recent developments in the field and some topics that are not commonly discussed in books devoted to ferroelectrics.

L. Pardo
J. Ricote

Contents

List of Contributors

Alfons Albareda
Applied Physics Department,
Universitat Politècnica de Catalunya,
08034 Barcelona,
Spain

K. Brebøl
Limiel ApS,
DK - 4772 Langebæk,
Denmark

Iñigo Bretos,
Instituto de Ciencia de Materiales de Madrid (CSIC),
Sor Juana Inés de la Cruz, 3,
Cantoblanco,
28049 Madrid,
Spain

A. J. Bushby,
Centre for Materials Research and School of Engineering and Materials Science,
Mile End Road,
London E1 4NS,
UK

Maria Elena Montero Cabrera
Centro de Investigación en Materiales Avanzados, S.C.
Miguel de Cervantes 120,
Complejo Industrial Chihuahua,
31109 Chihuahua,
Mexico

M. Lourdes Calzada
Instituto de Ciencia de Materiales de Madrid (CSIC),
Sor Juana Inés de la Cruz, 3,
Cantoblanco,
28049 Madrid,
Spain

D. Chateigner
Laboratoire de CRIstallographie et Science de MATériaux CRISMAT-ENSICAEN,
Institut Universitaire de Technologie (IUT),
Université de Caen Basse Normandie,
6 Boulevard du Maréchal Juin,
F-14050 Caen,
France

C. Chima-Okereke,
Centre for Materials Research and School of Engineering and Materials Science,
Mile End Road,
London E1 4NS
UK

Jiří Erhart
Department of Physics and International Centre for Piezoelectric Research,
Technical University of Liberec,
Studentská 2,
CZ-461 17 Liberec 1,
Czech Republic

Luis E. Fuentes-Cobas
Centro de Investigación en Materiales Avanzados, S. C.
Complejo Industrial Chihuahua,
Miguel de Cervantes 120,
31109 Chihuahua,
México

Francisco Montero de Espinosa Freijo
Instituto de Acústica,
Serrano 144,
28006 Madrid,
Spain

Carmen Galassi
Institute of Science and Technology for Ceramics ISTEC-CNR,
Via Granarolo, 64,
I-48018 Faenza (RA),
Italy

Janez Holc
Jožef Stefan Institute,
Jamova cesta 39,
SI-1000 Ljubljana,
Slovenia

B. Jiménez
Instituto de Ciencia de Materiales de Madrid (CSIC),
Consejo Superior de Investigaciones Científicas,
28049, Madrid,
Spain

R. Jiménez
Instituto de Ciencia de Materiales de Madrid (CSIC),
Consejo Superior de Investigaciones Científicas,
28049, Madrid,
Spain

Kazumi Kato
National Institute of Advanced Industrial Science and Technology (AIST),
2266-98 Anagahora,
Shimoshidami,
Moriyama-ku,
Nagoya 463-8560,
Japan

A. L. Kholkin
Departent of Ceramic and Glass Engineering, CICECO,
University of Aveiro,
Aveiro,
Portugal

Marija Kosec
Jožef Stefan Institute,
Jamova cesta 39,
SI-1000 Ljubljana,
Slovenia

Wolfgang Kreher
Institute for Materials Science,
Technische Universität Dresden,
Germany

Danjela Kuscer
Jožef Stefan Institute,
Jamova cesta 39,
SI-1000 Ljubljana,
Slovenia

Doru C. Lupascu
Institut für Materialwissenschaft,
Universität Duisburg-Essen,
Essen,
Germany

Christopher S. Lynch
Department of Mechanical and Aerospace Engineering,
University of California,
Los Angeles,
USA

L. Pardo
Instituto de Ciencia de Materiales de Madrid (ICMM-CSIC),
Cantoblanco,
28049 – Madrid,
Spain

Rafel Pérez
Applied Physics Department,
Universitat Politècnica de Catalunya,
08034 Barcelona,
Spain

M. J. Reece
Centre for Materials Research and School of Engineering and Materials Science,
Mile End Road,
London E1 4NS,
UK

Yago Gómez-Ullate Ricón
Instituto de Acústica,
Serrano 144,
28006 Madrid,
Spain

J. Ricote
Instituto de Ciencia de Materiales de Madrid (CSIC),
Sor Juana Inés de la Cruz 3,
Cantoblanco,
E-28049 Madrid,
Spain

W. L. Roberts
Centre for Materials Research and School of Engineering and Materials Science,
Mile End Road,
London E1 4NS,
UK

Jörg Schröder
Institute of Mechanics,
Universität Duisburg-Essen,
Essen,
Germany

V. V. Shvartsman
Angewandte Physik,
University of Duisburg-Essen,
Duisburg,
Germany

Ilona Westram
Institute for Materials Science,
Darmstadt University of Technology,
Darmstadt,
Germany

Chapter 1
Advances in Processing of Bulk Ferroelectric Materials

Carmen Galassi

1.1 Introduction

The development of ferroelectric bulk materials is still under extensive investigation, as new and challenging issues are growing in relation to their widespread applications. Progress in understanding the fundamental aspects requires adequate technological tools. This would enable controlling and tuning the material properties as well as fully exploiting them into the scale production. Apart from the growing number of new compositions, interest in the first ferroelectrics like $BaTiO_3$ or PZT materials is far from dropping. The need to find new lead-free materials, with as high performance as PZT ceramics, is pushing towards a full exploitation of barium-based compositions. However, lead-based materials remain the best performing at reasonably low production costs. Therefore, the main trends are towards nano-size effects and miniaturisation, multifunctional materials, integration, and enhancement of the processing ability in powder synthesis. Also, in control of dispersion and packing, to let densification occur in milder conditions. In this chapter, after a general review of the composition and main properties of the principal ferroelectric materials, methods of synthesis are analysed with emphasis on recent results from chemical routes and cold consolidation methods based on the colloidal processing.

1.2 Ferroelectric Materials

Ferroelectric materials are a subgroup of spontaneously polarised pyroelectric crystals, and are characterised by the presence of a spontaneous polarisation. This polarisation is reversible under the application of an electric field of mag-

Institute of Science and Technology for Ceramics ISTEC-CNR, Via Granarolo, 64, I-48018 Faenza (RA) Italy, Phone + 39 0546 699750, carmen.galassi@istec.cnr.ita

nitude less than the dielectric breakdown of the material itself [1, 2, 3]. Ferroelectric materials are divided into four categories: the perovskite group (ABO_3) that is the most important one, the bismuth layer structure group, the tungsten bronze group (Fig. 1.1) and the pyroclore group. Most ferroelectric materials undergo a structural phase transition from a high temperature paraelectric phase to a low temperature ferroelectric phase. The temperature of the phase transition is called the Curie temperature (T_C). In the ferroelectric state, the displacement of the central B ion, when an electric field is applied to the unit cell, causes the reversal of polarisation. The areas with the same polarisation orientation are referred to as domains, with domain walls existing between areas of unlike polarisation orientation. The switching of many adjacent unit cells is referred to as domain reorientation or switching. When this ionic movement occurs, it leads to a macroscopic change in the dimensions of the unit cell and the ceramic as a whole.

In ferroelectric ceramics, domains are randomly oriented and thus the net polarisation is zero because of their cancellation effect. Therefore, the as-prepared ferroelectric ceramics are neither piezoelectric nor pyroelectric. To show piezoelectric and pyroelectric properties, polycrystalline ferroelectric ceramics must be poled at a strong external DC electric field (1–10 kV/mm). This must also be done at elevated temperatures to make the domains more easily switchable.

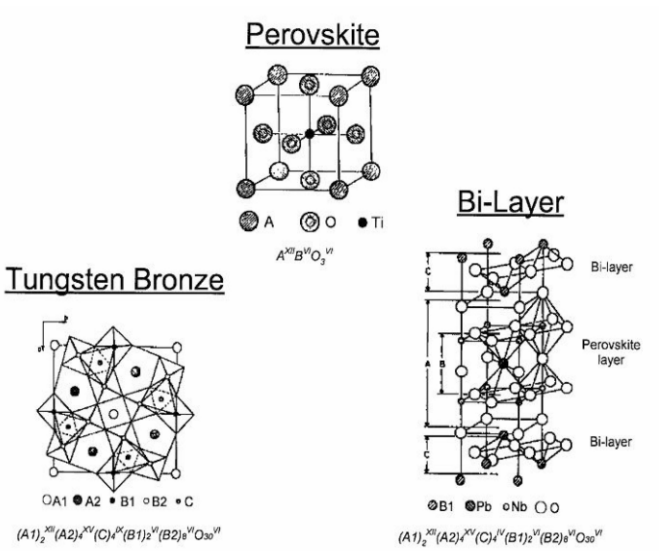

Fig. 1.1 Variants of the perovskite structure (from [4])

For a given composition, the T_C and the electrical, mechanical and optical properties strongly depend on the microstructure. This means density, grain size, shape, size distribution, porosity size and distribution, and anisotropy of grains or porosity. For most of the applications, fully dense materials are required to maximise the dielectric constant, the electrical breakdown strength, and the mechanical strength. These are also needed to minimise the dielectric loss tangent. Porosity is introduced in the materials, for example, when the reduction of the acoustic impedance is required. The value of the piezoelectric coefficients in ferroelectric materials at room temperature ranges from several pC N^{-1} in the $Sr_2Nb_2O_7$ family of layer structure perovskites, to more than 2000 pC N^{-1} in single crystals of relaxor-based ferroelectrics. This covers three orders of magnitude. Ferroelectricity was first discovered in the Rochelle salt (sodium potassium tartrate tetrahydrate, $KNa(C_4H_4O_6)_4H_2O$). But only after the discovery of ferroelectric ceramics, during the Second World War, did the number of applications grow rapidly.

1.2.1 Perovskite Type Materials

Perovskite crystals are represented by the general formula ABO_3 where the valence of *A* cations is from +1 to +3 and of *B* cations from +3 to +6. The perovskite unit-cell consists of a corner-linked network of oxygen octahedra, creating an octahedral cage (B-site), and the interstices (A-sites). Various A-site substitutions result in a large family of simple perovskite ferroelectrics (more than 100). In many ferroelectric ceramics, represented by the families of $BaTiO_3$ and lead-based solid solutions, Ti^{4+} (Zr^{4+}) ions occupy the B-site while Pb^{2+} (Ba^{2+}) ions occupy the A-site [4]. Variations of the corner linked octahedral-like tilt or rotations result in new families of ferroelectrics. Among those, the tungsten bronze and the bilayer structures are the most important (Fig. 1.1).

1.2.1.1 Barium Titanate

Barium titanate ($BaTiO_3$ or BT) [5] is a ferroelectric and piezoelectric material with a variety of commercial applications. These applications include multilayer ceramic capacitors (MLCCs), embedded capacitance in printed circuit boards, underwater transducers (sonars), thermistors with positive temperature coefficient of resistivity (PTCR), and electroluminescent panels. It shows relatively low T_C (120°C) and low electromechanical coupling factor (0.35). The grain size of $BaTiO_3$ plays a major role in ferroelectric properties. Much attention has therefore been paid to the synthesis of single-phase $BaTiO_3$ ceramics with a controlled microstructure (grain size > critical size). In addition, both stoichiometry and composition control are important parameters for the control of the ferroelectric properties [6]. $BaTiO_3$ is often combined with additives to modify and improve properties. Sr^{2+} reduces the T_C while Pb^{2+} increases it. Ca^{2+} enhances the temperature

range of stability of the tetragonal phase (T_C shifters are $SrTiO_3$, $CaZrO_3$, $PbTiO_3$, and $BaSnO_3$). Co^{2+} reduces the high electric field losses. For example, in the system $BaTiO_3$–$SrTiO_3$, the high *T*c value of pure $BaTiO_3$ ceramics can be decreased by increasing the Sr content. The dependence of the permittivity on the electric field can also be accurately tailored (tunability). The barium strontium titanate solid solutions ($Ba_xSr_{1-x}TiO_3$ or BST) are then very attractive for tunable resonators, filters, phase-shifters and variable frequency oscillators.

Depressors, such as $Bi_2(SnO_2)_3$, $MgZrO_3$, $CaTiO_3$, $NiSnO_3$, and the shifters, are added in small (1–8 wt%) quantities to the base $BaTiO_3$ composition. This is to lower or depress the sharpness of the dielectric constant peak at the T_C, thus giving a flatter dielectric constant–temperature profile.

Solid solutions of $BaTiO_3$ and non-ferroelectric $BaSnO_3$, $Ba(Ti_{1-x}Sn_x)O_3$ (BTS) exhibit ferroelectric properties. These are used for capacitors and ceramic boundary layer capacitors, bolometers, actuators and microwave phase shifters [7]. In BTSx ceramics, the isovalent Sn-substitution on the Titanium (Ti) site makes it possible to reduce the temperature dependence. It is also possible to control the room-temperature values of macroscopic properties, such as dielectric characteristics, relaxor behaviour, and sensor performance. With increasing Tin (Sn) content between 10% and 20%, the Tc of the paraelectric–ferroelectric phase transition decreases considerably. For x >0.05, deviations from the Curie–Weiss law for the temperature dependence of the permittivity increase significantly. The phase transition of BTSx becomes increasingly diffuse.

1.2.1.2 Lead-Based Materials

Lead Titanate ($PbTiO_3$ or PT) is a ferroelectric material with a phase transition temperature of 490°C. It has unique properties like high transition temperature, low dielectric constant, low ratio for the planar-to-thickness coupling factor, and a low aging rate of the dielectric constant. PT ceramics are good candidates as stable pyroelectric and piezoelectric devices for high temperature or high frequency applications. Anisotropic thermal expansion during cooling from a high sintering temperature creates large internal stresses in the material, which is destroyed by microcracking. The expansion is caused by the phase transition from cubic paraelectric to tetragonal ferroelectric (with a relatively large c/a ratio of ~1.065). Therefore, PT materials can be prepared via the conventional solid state reaction only after modification with proper dopants.

Lead Zirconate Titanate ($Pb(Zr_xTi_{1-x})O_3$ or PZT) ceramics [8], solid solutions of PT and $PbZrO_3$ (PZ) possess high electromechanical coupling coefficients (K_p=0.70). They have higher T_C values than $BaTiO_3$, which permit higher operation and processing temperatures. They can be easily poled. They possess a wide range of dielectric constants. They are relatively easy to sinter. And, most important, they form solid-solution compositions with many different constituents. This allows a wide range of achievable properties. Although PZT ceramics of

different compositions have various functions, a salient feature of the phase diagram for this solid solution system is the existence of the almost temperature-independent phase boundary around x = 0.52–0.53. This separates a rhombohedral Zr-rich phase from a tetragonal Ti-rich phase. The dielectric constant, piezoelectric constant and electromechanical coupling coefficient exhibit a pronounced maximum value for the composition corresponding to this phase boundary. This is generally referred to as the morphotropic phase boundary (MPB). The position of the MPB is not exactly defined as it is associated to a phase coexistence region for which different models have been proposed: coexistence of the two phases, metastability of one of two phases, and unwanted compositional fluctuations [9]. An inversely proportional dependence of the width of the coexistence phase was proposed on the grain size [10] as the result of the thermal fluctuations during cooling. Recently, for compositions close to the MPB, the existence of a low symmetry monoclinic (M) phase bridging the tetragonal (T) and rhombohedral (R) ones was revealed in the temperature range 20-300K [11]. The T–M transition gradually changes from first to second order increasing the Ti content from the boundary with the R phase to x = 0.48. This confirms that the coexistence of T and M phases is intrinsic and not due to compositional fluctuations [12]. The PZT materials are almost always used with a dopant, a modifier, or other chemical constituents to tailor their basic properties to specific applications. Donor doping (Nb^{5+} replacing Zr^{4+} or La^{3+} replacing Pb^{2+}) increases the electrical resistivity of the materials by at least three orders of magnitude. The donors are usually compensated by A-site vacancies. These additives (and vacancies) enhance domain reorientation. Ceramics produced with these additives are characterised by high dielectric constants, maximum coupling factors, square hysteresis loops, low coercive fields, high remnant polarisation, higher dielectric loss, high mechanical compliance, and reduced aging. Acceptor doping (Fe^{3+} replacing Zr^{4+} or Ti^{4+}) is compensated by oxygen vacancies and usually has limited solubility in the lattice. Domain reorientation is limited. Hence, ceramics with acceptor additives are characterised by poorly developed hysteresis loops, lower dielectric constants, low dielectric losses, low compliances, and higher aging rates. Further, the substituting ions can be of the same valency and approximately the same size as the replaced ion. Isovalent substitution such as Ba^{2+} or Sr^{2+} replacing Pb^{2+} or Sn^{4+} replacing Zr^{4+} or Ti^{4+}, usually produce inhibited domain reorientation and poorly developed hysteresis loops, lower dielectric loss, low compliance, and higher aging rates.

Lead Lanthanum Zirconate Titanate (PLZT) ceramics, with variable lanthanum concentrations and different Zr/Ti ratios, exhibit a variety of ferroic phases and embrace all compositional aspects of the dielectric, piezoelectric, pyroelectric, ferroelectric, and electro-optic ceramics. The addition of lanthanum lets the system maintain extensive solid solution. It also decreases the stability of the ferroelectric phases in favour of the paraelectric and anti-ferroelectric phases. T_C reduces with increasing lanthanum. At a 65/35 ratio of Zr/Ti, a concentration of 9% lanthanum (designated as 9/65/35) is sufficient to reduce the temperature of the

stable ferroelectric polarisation to slightly below room temperature. This results in a material that is non-ferroelectric and cubic in its virgin state. The cross-hatched area existing along the FE–PE phase boundary denotes a region of diffuse, metastable relaxor phases that can be electrically induced to a ferroelectric phase. Materials within this region exhibit electro-optic behaviour.

1.2.1.3 Relaxor Ferroelectrics

Some ferroelectric ceramics exhibit significantly large electrostrictive effect mostly just above their Tc. This effect is where an electric field can enforce the energetically unstable ferroelectric phase related to the presence of nanoscale ordered regions in a disordered matrix [13]. This effect is utilised in relaxor ferroelectrics (RFE) that show extraordinarily high dielectric constants and a diffuse Tc in a moderate temperature range. Among those materials, lead magnesium niobate $Pb(Mg_{1/3}Nb_{2/3})O_3$ (PMN) based relaxor ceramics have been thoroughly investigated. They have been successfully applied as high-strain (0.1%) electrostrictive actuators and high dielectric constant (>25 000) capacitors. The most popular specific composition in this system is PMN–0.1PT. This increases the T_m (the temperature of maximum dielectric constant for relaxors, equivalent to T_C for normal ferroelectrics) of PMN to ~40°C. For this composition, the temperature of polarisation loss (T_d) is ~10°C. Hence, the material is a relaxor at room temperature (25°C). An addition of ~28% PT causes the material to revert to a normal ferroelectric tetragonal phase with T_C ~130°C.

1.2.1.4 Alkaline Niobates

Alkaline niobates are one of the families of materials under investigation as a possible alternative to lead-based piezoelectric materials [14]. In Fig. 1.2, the Tc against the piezoelectric constant is reported for comparison with PZT and other lead-free materials.

Potassium niobate ($KNbO_3$) (KN) exhibits the same sequence of phase transitions as $BaTiO_3$. These transitions are from the cubic paraelectric to the tetragonal phase at 435◦C, from the tetragonal to the orthorhombic phase at 225°C, and from the orthorhombic to the rhombohedral phase at −10°C. The tetragonal, orthorhombic and rhombohedral phases are all ferroelectric. Potassium niobate ceramics exhibit weak piezoelectric properties. Solid solutions of $KNbO_3$ with $NaNbO_3$ (NN) lead to a system with many MPBs, showing ferroelectricity up to about 90% $NaNbO_3$. $K_{0.5}Na_{0.5}NbO_3$ (KNN) [15] ceramics, fabricated by conventional sintering, show relatively good piezoelectric properties (Table 1.1). Further improvement of the properties is being made by continuous improvement of processing routes for powder preparation, doping, shaping and sintering methods.

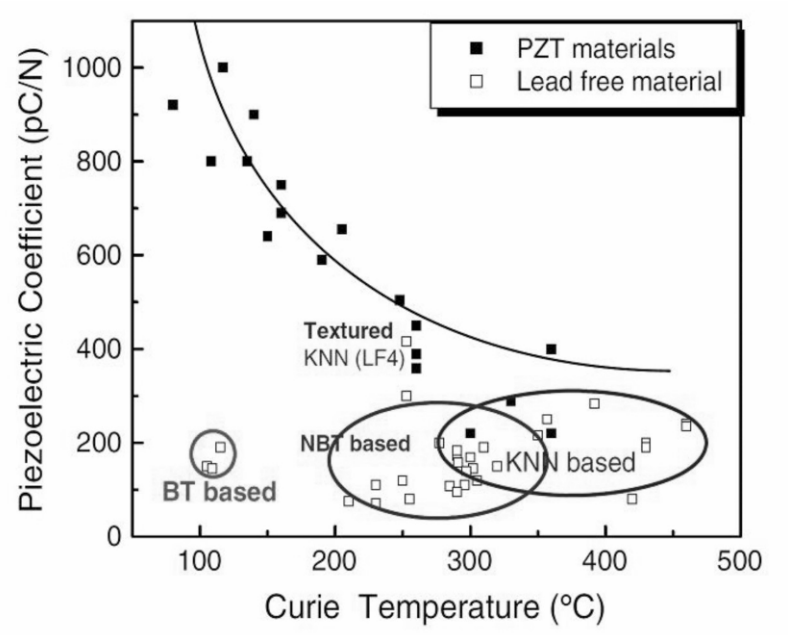

Fig. 1.2 Room temperature values of d_{33} as a function of T_C for various Piezoceramics (from [14]).

1.2.1.5 Bismuth-Based Materials

Bi-based compounds have similar or larger levels of ion off-centering than Pb-based compounds, leading to large ferroelectric polarisations [16]. In addition, they have considerably higher transition temperatures to the paraelectric phase. This results in reduced temperature dependence of the properties under room-temperature operating conditions [17]. $(Bi_{0.5}Na_{0.5})TiO_3$ (BNT) is the most important among the bismuth containing ferroelectric perovskites. The BNT ceramic exhibits a large remnant polarisation, a Curie temperature Tc=320°C and a phase transition point from ferroelectric to anti-ferroelectric Tp=200°C. However, data on piezoelectric properties of the BNT ceramic are scarce because it is difficult to pole this ceramic with its large coercive field, (Ec=73 kV/cm). Therefore, BNT-based solid solutions that can be poled easily have recently been studied. Particularly, a large piezoelectricity is expected for the BNT-based solid solutions with a morphotropic phase boundary (MPB). A morphotropic phase boundary separating ferroelectric tetragonal and rhombohedral phases exists in the $Na_{0.5}Bi_{0.5}TiO_3$-$BaTiO_3$ and related ternary system with $K_{0.5}Bi_{0.5}TiO_3$ [18, 19]. In Table 1.1, the main piezoelectric properties of some representative PZT materials are reported for comparison with lead-free materials.

Table 1.1 Comparison of the properties of some lead-based and lead-free materials (elaborated from [14]).

Material	T_C (°C)	ε_r	Loss	k_{33}	d_{33} (pC/N)	g_{33} (10^{-3} Vm/N)	E_C (kV/cm)	Q
PZT4	328	1300	0.004	0.70	290	25	~18	>500
PZT5A	365	1700	0.02	0.71	375	25	~15	75
PZT8	300	1000	0.004	0.64	225	25	~22	>1000
PZT5H	190	3400	0.02	0.75	590	20	6–8	65
KNN	420	290	0.04	0.51	80			130
$BaTiO_3$	135	1420		0.49	191			
BNBT6	288	580		0.55	125			81

1.2.2 Aurivillius Ceramics

Aurivillius phases are generally described by the general formula $(Bi_2O_2)^{2+}$ – $(A_{n-1}B_nO_{3n+1})^{2-}$. A_{n-1} is a mono, divalent or trivalent cation 12-coordinated. B is a quadri, penta, or hexavalent metal ion octahedrally coordinated. *n* is an integer representing the number of perovskite layers and can range from 1 to 8 [20]. These bismuth layer-structured ferroelectric (BLSF) compounds, first studied by Aurivillius, belong to the family of bismuth titanate ($Bi_4Ti_3O_{12}$ or BiT) [21]. Except for BiT that is monoclinic, they possess pseudoperovskite layers ($A_{n-1}B_nO_{3n+1}$) $^{2-}$ stacked between $(Bi_2O_2)^{2+}$ layers (Fig. 1.1). They are of great interest due to their high Curie temperatures (up to 980°C) and good piezoelectric properties. Several critical issues concern the processing, like reproducibility of the properties, narrow range of sintering temperature. Due to the layer structure, the compositions exhibit a very high anisotropy of properties [15]. The microstructure of such ceramic materials consists of plate-like shaped grains. From the point of view of piezoelectric properties, $SrBi_4Ti_4O_{15}$ (SBiT) is of special interest because of its high Curie temperature (~530°C) and its remarkably stable properties on the driving field amplitude and frequency [22]. Wang *et al*. [23] recently succeeded in producing Potassium Bismuth Titanate ($K_{0.5}Bi_{4.5}Ti_4O_{15}$) ~95% dense with Tc= 555°C, Qm 1602 and d_{33}= 21.2 pC/N. Mixed Aurivillius phases are of interest for their potentially enhanced properties [24].

1.2.3 Tungsten Bronze Ceramics

Tungsten bronze (TB) type ferroelectric materials exhibit interesting electro-optic, non-linear optic, piezoelectric and pyroelectric properties. TB structure has a general formula of $(A1)_4(A2)_2(C)_4(B1)_2(B2)_8O_{30}$. B-type cations occupy A1, A2 and C sites. B-type cations occupy the B1 and B2 octahedral sites [25]. In the formula,

A1, A2, C, and B are 15-, 12-, 9- and 6-fold coordinated sites in the crystal lattice structure (Fig. 1.1). Generally, A1 and A2 sites can be filled by Na, Li, K, Ca, Sr, Ba, Pb, Bi and some rare earth (Sm, Nd, Dy, Ce) cations. B1 and B2 sites can be filled by W, Nb, Ta. The smallest interstice C is often empty, and hence a formula is $A_6B_{10}O_{30}$ for the filled TB structure. The metal cations distribution in the different sites of the TB structure plays a crucial role in tailoring physical and functional properties. Moreover, the properties of the TB structure could be modified in a wide scale, by coupling the most important members of the TB family. These members are barium sodium niobates (BNN), potassium lanthanum niobates (KLN), strontium barium niobates (SBN), strontium sodium niobates (SNN), etc. $PbNb_2O_6$ (PN) with a Curie temperature close to 570°C is ferroelectric orthorhombic for sintering temperature above 1250°C. It can be obtained in a single phase only upon appropriate thermal treatments [26].

1.2.4 Pyrochlore

The pyrochlore structure is shown by materials of the stoichiometry $A_2B_2O_7$. B is a tetravalent or pentavalent species and A trivalent or divalent, respectively [27]. Cadmium pyroniobate, $Cd_2Nb_2O_7$ (CNO) is ferroelectric at low temperatures. It exhibits three dielectric anomalies in the narrow temperature range from 195 to 205K, above which it is cubic [28]. The ferroelectric behaviour disappears above 185K, and at the same temperature there are anomalies in the dielectric constant and specific heat [29]. The pyrochlore structure is commonly described as composed of two interpenetrating networks without common constituents. The frequency dependence of the dielectric constant in this temperature regime is similar to that seen in typical relaxor materials. This indicates the presence of polar clusters in CNO.

1.2.5 Multiferroics

Recently, materials that combine ferroelectric and magnetic properties are triggering scientific and technological interest for application in novel multifunctional devices [30]. Multiferroics and magnetoelectric materials can be single phase or two phase materials where magnetisation can be induced by an electric field and electrical polarisation can be induced by a magnetic field. Single phase materials include the anti-ferromagnetic relaxor ferroelectrics like $Pb(Fe_{1/2}Nb_{1/2})O_3$ (PFN) and $Pb(Fe_{1/2}W_{1/3})O_3$ (PFW). They are also orthorhombic manganites, $REMnO_3$ or $REMn_2O_5$, where RE is a rare earth element, $LiCoPO_4$ and $BiFeO_3$, and its solid solutions with $BaTiO_3$ [31]. Indirect coupling, via strain, between two materials such as a ferromagnet and a ferroelectric can be introduced because of the low value of the magnetoelectric coefficient or the low temperature range of the mag-

netoelectric effect. Intimate contact between a piezomagnetic (or magnetostrictive) material and a piezoelectric (or electrostrictive) material can be achieved in the form of composites [32]. Particulate ceramic composites have been studied by combining BT and ferrites like $(Ni(Co,Mn,Zn)Fe_2O_4–BaTiO_3$ [33], $CoFe_2O_4–BaTiO_3$ [34] $NiFe_2O_4–BaTiO_3$, $LiFe_5O_8–BaTiO_3$, or PZT and ferrites like $NiFe_2O_4$–PZT, $(Ni,Zn)Fe_2O_4$–PZT, $CuFeCrO_4–BaPbTiO_3$, or $CoFe_2O_4–Bi_4Ti_3O_{12}$, or laminates (as PZT or PMN-PT) with high magnetostrictive materials, such as Ni–Co–Mn ferrite (NCMF) [35].

1.3 Powder Synthesis

1.3.1 Solid State Reaction (SSR)

The most commonly used process for the powder synthesis is based on the thorough mixing of the starting oxides or carbonates. This is followed by solid-state reaction at high temperatures. The successful production of powders for advanced electronic ceramics depends on the control of the synthesis parameters and purity and morphology of the raw materials.

1.3.1.1 Barium Titanate

Barium titanate (BT) is produced from the reaction between TiO_2 and $BaCO_3$ [36]. The reactants are mixed in order to reduce agglomerates, to increase the homogeneity and to reduce the particle size. After mixing, the raw materials are treated at high temperatures and then, the $BaTiO_3$ is produced. According to Beauger *et al.* [37], the reaction between $BaCO_3$ and TiO_2 proceeds through the following stages:

1. Formation of $BaTiO_3$ at the expense of TiO_2:

$$BaCO_3 \rightarrow BaO + CO_2 \quad (1)$$

$$BaO + TiO_2 \rightarrow BaTiO_3 \quad (2)$$

The reaction proceeds rapidly at the surface of contact between the reactants.

2. When $BaTiO_3$ is formed at the surface, the reactants are separated by a product layer; then the course of the reaction becomes diffusion-controlled. Barium ions must diffuse through $BaTiO_3$ and penetrate into TiO_2 grains. However, when reaching the $BaTiO_3$ interface, barium can react according to:

$$BaTiO_3 + BaO \rightarrow Ba_2TiO_4 \quad (3)$$

Hence, the formation of Ba_2TiO_4 proceeds by the reaction between BaO and the prior-formed $BaTiO_3$.

3. Finally, TiO_2 and Ba_2TiO_4 react to produce $BaTiO_3$, which is the final phase:

$$Ba_2TiO_4 \rightarrow BaTiO_3 + BaO \quad (4)$$

$$TiO_2 + BaO \rightarrow BaTiO_3 \quad (5)$$

To obtain single-phase $BaTiO_3$, temperatures above 900°C are required and the powders are often aggregated. This affects the grain growth during sintering. In order to avoid or minimise this problem, it is important to select an appropriate milling method and control the chemical impurities introduced into the powders from the grinding medium (Al_2O_3, ZrO_2, etc.). Moreover, it is difficult to mix and to maintain chemical homogeneity in the final product, especially when one of the reactants is present in a minor proportion. Small-grained and well-crystallised pure ferroelectric materials are often required as a consequence of the evolution towards miniaturisation, while keeping the highest dielectric constant and low production costs. Therefore, a renewed interest into the formation of BT nanoparticles by a solid state reaction has grown recently [38]. By a solid-state reaction at 700°–800°C of mixtures of nanocrystalline raw materials, Buscaglia *et al.* [39] obtained single-phase $BaTiO_3$ powders with a specific surface area up to 15 m^2/g (particle size: 70 nm). This resulted in highly dense materials after sintering. When nanocrystalline $BaCO_3$ and TiO_2 are chosen as starting powders, they react directly at a temperature lower than the air decomposition of $BaCO_3$. This prevents the formation of the side product Ba_2TiO_4. The same group developed a two-step method for the fabrication of hollow $BaTiO_3$ ferroelectric particles [40]. It involves the suspension of barium carbonate powder in the aqueous solution of peroxy titanium. Amorphous titania precipitates on the barium carbonate crystals by slowly heating the suspension up to 95°C and keeping the temperature constant for five hours. The resulting $BaCO_3@TiO_2$ core–shell particles are then converted into $BaTiO_3$ hollow particles by calcination at 700°C. The out-diffusion of the core phase is faster than in-diffusion of the shell. This leads to the formation of the cavity in the material. Initially, the strong imbalance of the diffusion fluxes determines the formation of Kirkendall porosity close to the original $BaCO_3/TiO_2$ interface without intermediate decomposition. Here, the $BaCO_3$ crystals behave as sacrificial templates. The starting $BaCO_3$ elongated crystals produced empty shells with an average thickness of about 70 nm composed of equiaxed nanocrystals. The size of the core crystals and the reaction temperature are critical in the solid-state fabrication of hollow structures. Calcination at 900–1000°C results in the collapse of the empty shell, with the formation of aggregates of small $BaTiO_3$ particles.

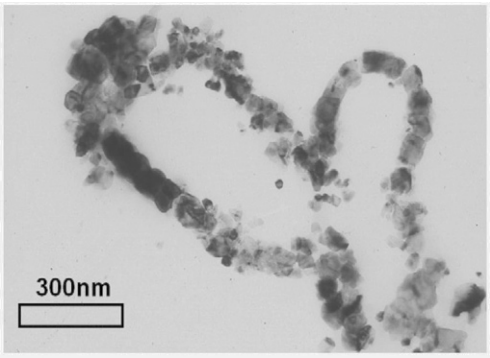

Fig. 1.3 TEM image of the cross-section of $BaTiO_3$ hollow particles obtained after 24 h calcination at 700°C of the $BaCO_3$@TiO_2 powder (from [40]).

$BaTiO_3$ is a stable perovskite end member and is a good candidate to produce lead-free materials. This is because of its high degree of solubility into other perovskite phases forming solid solution [41], and its stable tetragonal crystal structure at room temperature. A few examples are $Bi(Zn_{1/2}Ti_{1/2})O_3$–$BaTiO_3$ [42], $CaTiO_3$–$BaTiO_3$ [43], $BaTiO_3$– $Ba_5Nb_4O_{15}$ [44].

1.3.1.2 Lead-Based Perovskites

PZT powders are still mostly produced by the conventional mixed-oxide route [8]. This has been extensively investigated for compositions close to the MPB. The investigations were to enable an understanding of how the processing parameters and the dopants added affect the compositional fluctuations and phase coexistence. As in the binary mixtures, PT is formed firstly (450°-600°C) with an exothermic reaction and a large volume expansion. PZ is formed at 700°-800°C with endothermic reaction and large volume increase. The formation of the PZT solid solution [45] proceeds with expansion of more that 12% depending on the particle size [46,47]. Therefore, direct reaction sintering is not a means to obtain dense materials. Owing to the enlarged phase coexistence region [48], the equilibrium state is not reached in the calcined powders, even for long heat treatments. This results in poor reproducibility of the process. Moreover, even if the as-reacted powders consist of a mixture of phases, where the degree of homogenisation of the starting oxides depends on the milling conditions [49], reactivity and dispersion of the raw materials [50, 51], they homogenise at the sintering temperature and form monophase materials. A recent study [52], in terms of mutual interaction of the phases in the composition PZT53/47 calcined at 1000°C, confirms the presence of the rhombohedral phase in the calcined powders. The materials are generally prepared by homogenisation and milling of the starting oxides in a liquid media, drying and calcination at temperatures between 600°C and 900°C. A two-stage solid state reaction (reactive calcination) has been developed for PZT ceramics to achieve finer-grained starting powder. The method is based on a

pre-reaction of ZrO_2 and TiO_2 at high temperature (1400°C) to form a rutile structure. This exploits the molar volume expansion of the B-site precursor phase. PbO is then added to form the perovskite [53,54]. Being mechanically weak calcined agglomerates, as a consequence of the volume expansion, they are fractured in nano-sized particles (70 nm) by high energy milling. The powder can be densified at 950-1000°C to obtain grain size in the range 0.1 to 10 μm [55]. The milling step becomes more critical when dopants are added or multicomponent compositions are produced. Galassi *et al.* investigated the influence of milling introduced at different steps of the powder treatments (Table 1.2), on the microstructure and dielectric and piezoelectric properties of a multicomponent complex PZT system ($[Pb(Li_{0.25}Nb_{0.75})]_{0.06}$ O_3-$PMN_{0.06}$-$PZT_{0.88}$) [56]. Simple milling in agata mortar or long ball milling of the raw materials altogether, or pre-grinding of the coarser oxide, resulted in sintered materials with comparable density but different microstructure and quality factor (Q_m) ranging from 380 to more than 2000.

Table 1.2 Density and piezoelectric properties of the PZT samples (elaborated from [56]).

Sample	Grinding procedure	Green Density (%)	Sintered Density (%)	k_p	d_{31} (10^{-12}m/V)	Q_m
A	Agate mortar, after calcination	64.2	99.7	0.32	-50.0	380
B	Wet milling for 100 h, after calcination	60.4	100.0	0.54	-64.7	2132
C	Sample A, with pre-ground MnO_2	57.4	99.5	0.54	-69.0	994

In the solid state synthesis of PMN powders, the formation of lead niobate based pyrochlore is a critical issue. Among the several methods of powder preparation developed to reduce the undesirable pyrochlore phase, the process that has been more successful is the so-called columbite precursor method [57]. In this technique, MgO and Nb_2O_5 are first reacted to form the columbite structure ($MgNb_2O_6$), with high volume expansion. This is then reacted with PbO and eventually TiO_2 to form the PMN or PMN–PT compositions. Recently, Kwon *et al.* [58] produced 0.65PMN-0.35PT by reactive calcination of precursor mixture of fine and coarse raw materials after prolonged milling.

Lead Metaniobate ($PbNb_2O_6$) has been produced by SSR [26] by adding excess PbO to the nominal formula as the required calcining temperature is 1050°C and the sintering one is higher than 1250°C, to avoid the formation of the low temperature rhombohedral structure. For polycrystalline PN materials, obtaining a single orthorhombic phase is a difficult task. Generally, these materials are formed from a mixture of rhombohedral and orthorhombic phases. Nevertheless, an appropriate thermal treatment followed by rapid cooling can yield a PN material with a single orthorhombic phase.

Microwave irradiation of reactants is a means of accelerating a variety of chemical reactions and to lower the reaction temperature [59, 60]. Microwave heating is affected by mainly two factors; permittivity (dielectric constant) (ε′), and dielectric loss (ε″) [61]. The dependence of the heating rate is given by (ε′/ε″), defined as loss tangent (tan δ). The dielectric loss tangent (tan δ) depends on the temperature, composition, and physical state of the reactants and the frequency of the electromagnetic waves. Single phase PZT at temperature as low as 600°C can be obtained by microwave-assisted SSR procedure with enhancement of the reaction rates if one of the constituent precursors is a non-stoichiometric oxide [62].

1.3.2 Mechanochemical Synthesis

It consists of the activation of the reactions of the oxide precursors by mechanical energy rather than heat energy, like in the conventional SSR. The main issue is that it skips the calcination step leading to nano-sized powders with better sinterability. Kong *et al.* recently published a comprehensive review on this technique [63] where they show many successful examples of the production of ferroelectric powders via the high energy mechanical milling. They did this by direct synthesis of compounds, mainly in the PT, PZT, PLZT, PMN, and PZN, PFW and BiT systems, or by improved reaction, to form BT, or by amorphisation of precursors for Aurivillius family compounds. Different equipments are used including vibration shake mills, planetary mills or attritor mills. Important parameters are the type of mill, the materials used for the milling vial and media, the milling speed and time, ball to powder weight ratio (BPR), milling environment, process additives, temperature control and the application of an electrical or magnetic field during milling. The comparison of planetary mill and shaker mill for the activation of PZT 53/47 powder in different conditions [64] showed that the BPR has a marked influence on the phase formation. Under a certain value, even prolonged (120 h) milling does not cause the formation of the single perovskitic phase. BPR of 20 at 500 rpm were the necessary conditions for the planetary mill to produce the single phase after 65 hours. This suggests that the milling intensity is related to the shock power injected on the mass of powder trapped in the collision. This could be related to localised temperature increase in the collision point that influences the rate of grain boundary and lattice diffusion processes. In the early stage of milling, the starting oxide powders are refined in both particle and crystallite size. A certain degree of amorphisation takes place that is lower at the higher BPR and milling speed. The mechanical activation makes dynamic processes of the diffusion and atomic rearrangements, enhanced by repeated fracturing and rebinding. Rojac *et al.* [65] proposed the use of a milling map as a tool for determining the critical or minimum cumulative kinetic energy for the formation of the amorphous phase or the intermetallic compound. This was to compare different milling equipments or process conditions. They designed and tested low energy and high energy milling experiments and showed that a critical cumulative kinetic

energy between 7 and 12 kJ/g is necessary to induce the formation of $NaNbO_3$. This milling energy strongly changes for different compositions up to values as high as 150 kJ/g. By mechanochemical synthesis, Xue *et al.* synthesised the PZT 52/48 single phase at room temperature [66] after 20 hours shaking at 900 rpm (SPEX shaker-mill) of the pre-ball milled mixture of the starting oxides. The fine powders partially mechanically activated for 10 hours show high sinterability [67]. Single phase PMN-PT ceramics at different PT content were produced in batches of 200 g each by mechanically activating the whole mixture of the starting oxides or by pre-activating two of the starting powders. The different particle size distribution influenced the final microstructure [68].

An amorphous mixture of Aurivillius compounds of the composition $(Bi_3TiNbO_9)_x(SrBi_2Nb_2O_9)_{1-x}$ with x=1.00, 0.65 and 0.35 was obtained upon mechanical activation for 336 hours in a vibrating mill Fritsch Pulverisette [69], of the starting materials that are transformed in the Aurivillius structure at 600 °C. This is a considerably lower temperature than the one needed in the conventional process. The highly reactive powder can be sintered at 1000°C or even at 700°C by hot pressing. Even $Bi_4Sr_{n-3}Ti_nO_{3n+3}$ compounds at increasing n become amorphous after 168 hours mechanical activation in vibration mill [70].

1.3.3 Chemical Methods

Several wet chemical routes are investigated to produce ultrafine starting powders, with improved chemical homogeneity, reduced agglomerate hardness and higher reactivity. They are transformed in the single phase at lower temperature, and result in better control of the stoichiometry and of the final material microstructure. Methods based on precipitation-filtration, such as co-precipitation and hydrothermal or sol-gel synthesis, were extensively applied.

1.3.3.1 Co-Precipitation

PZT and PZT-based powders and their composition modifications with one and more dopants have been produced by co-precipitation routes. The lower calcination temperature of powders produced by hydroxide and oxalate co-precipitation was shown to have strong effects on the sintered material [71]. Non-stoichiometric $PbTiO_3$ perovskites were obtained when an initial equimolar mixture of both oxides precursors was used [72]. Based on solubility calculations, Choy [73] analysed the optimum co-precipitation conditions to obtain PZT 52/48 from metal hydroxides precipitation. He found consistent experimental results (homogeneous precipitation at pH 9 and single perovskitic phase on heating at 900°C for two hours). Optimising the calcination temperature at 500°C, PZT 52/48 powder pellets, isostatically pressed, were densified in one step at 1050°C [74]. A two-step method was investigated to produce $(PbLa)(ZrSnTi)O_3$

composition, by adding the solution of the (Pb,La) ions to the as-washed (ZrSnTi) precipitates [75].

Residual alides when metal chlorides were used proved detrimental for the final properties of the materials. The peroxide-based route was proposed as an alternative method. Camargo [76] proposed the dissolution of Ti metal in the hydrogen peroxide and aqueous ammonia solution to form the peroxotitanato solution. Lead nitrate and zirconil nitrate solutions are added to this. PZT 53/47 coprecipitated starting from nitrites by using urea directly crystallises at 550°C [77]. Fine-grained $BaTi_{0.87}Sn_{0.13}O_3$ (BTS13) powder was synthesised from an oxalate precursor and used to prepare sintered ferroelectric BTS13 ceramics [78]. The precipitate powders show the coexistence of the BTS13 and $BaCO_3$ phases at heating till 1100°C, and the pure BTS13 phase at 1300°C. A small dielectric loss and low frequency dispersion of dielectric characteristics were found owing to high permittivity of the very fine particles. The BTS13 ceramic showed a diffuse paraelectric–ferroelectric phase transition due to the Sn substitution on Ti-sites and the fine grain size of the material. The advantages of this technique used to prepare BTS13 solid solution powder are the mild sintering conditions needed to densify.

1.3.3.2 Sol-Gel Synthesis

Sol-gel processing is widely used to synthesise multicomponent oxides with an intermediate stage including a sol or a gel state. It is a colloidal route based on the hydrolysis/condensation reaction of metal alcoxide salts or complexes (metal carboxilate complexes). Despite the potential for cation mixing at the molecular level, gels usually do not directly crystallise into the equilibrium oxide phase. However, intermediate phases are formed that require high temperature solid state reaction to form the pure phase systems [79]. From the analysis of the local structure of partially heat treated gels [80], it was found that heterogeneity exists at the molecular level. This is related to differences in the hydrolysis and condensation rates of alkoxides of different metals. Carboxylate gels involve the reaction of metal cations with carboxylate ligands to form carboxylate complexes, depending on the nature of the ligand, pH and temperature that form a crosslinked network. The carboxylate complexes and their subsequent crosslinking are formed as a result of deprotonation, complexation and polymerisation sequence. The rise of viscosity during concentration of the solution prevents the precipitation of the metal carboxylate complexes.

In order to keep as low as possible the amount of free metals in the solution, an excess of chelating agent is necessary. Large constant complex formation is preferable. Citric acid has been used as a chelating agent for barium and lead oxide and their multicomponent systems. The citrato-metal complexes are commonly used because they are stable to hydrolysis and ionically crosslink in concentrated solution. This prevents precipitation during gelation. Excess ligand and pH control are necessary to form homogenous gel. During the gel thermolysis, several reac-

tions take place. These can be discerned in scission of the different bonds in the amorphous gel at T<300°C and decomposition of the carboxylato-metal bonds at higher temperature, which gives rise to the formation of the oxide. Phase separation [79] can arise owing to the different thermal stability of the bonds or to the formation of carbonates with the decomposition products. During crystallisation, an intermediate pyrochlore phase is often formed before the formation of the stable perovskitic phase. This is attributed to the pyrochlore's higher nucleation site density and is related to its much disordered structure in comparison with the perovskite phase. The sol-gel chemistry, combined with the combustion process, leads to homogeneous, fine and highly reactive powders in a shorter time and at lower temperatures than traditional processes. Many nitrate citrate gels, when heated on a hot plate, burn in a self-propagating reaction, thus converting the precursor mixture directly into the products.

1.3.3.3 Self-Combustion Synthesis

The self-combustion synthesis technique consists in the heating of a saturated aqueous solution or gel of the desired metal salts or complexes, and a suitable organic fuel to boil. This is done until the mixture ignites and a self-sustaining and rather fast combustion reaction takes off. This results in a dry, usually crystalline, fine oxide powder. It exploits an exothermic, usually very rapid and self sustaining redox-type chemical reaction. The heat required to drive the chemical reaction is provided by the reaction itself. The combustion of metal nitrates-urea mixtures, for example, usually occurs as a self-propagating and non-explosive exothermic reaction. The large amounts of gases formed can result in the appearance of a flame that can reach temperatures up to 1000°C [81]. It shows many advantages (inexpensive precursors, short preparation time, modest heating, and simplicity). The main parameters that affect the course of the reaction are composition of starting mixture (fuel to oxidiser ratio), pH of the sol, modality of gel formation, and starting combustion temperature. Aqueous-based citrate-nitrate sol-gel combustion process can be adopted to reduce the reaction and sintering temperatures, and to improve chemical homogeneity in PZT bulk materials. The presence of nitrate ions is fundamental to the desired oxidation-reduction reaction. In this case, the exothermic reaction between the citrate as organic fuel and the nitrates as oxidiser can be initiated in a muffle furnace or on a hot plate at temperature lower than 500ºC. Banerjee [82] synthesised free standing nanocrystalline PZT 52/48 particles using this method. He found that the increase of the citrate to nitrate ratio (C/N) enhances the coagulation of particles and tends to form nanoporous particles. Niobium-doped lead zirconate titanate of the composition titanate (PZTN) precursor solution was prepared starting from Zr-oxynitrate, Pb-citrate, Nb- and Ti-peroxo-citrate precursors [83]. Citric acid monohydrate was the source of citrate anion that was used as both a chelating agent for metal cations and a fuel for combustion. The combustion reactions are highly exothermic (Fig. 1.4). They are autocatalytic in nature and lead to the complete decomposition of the organic com-

compounds. There is also a slow crystallization of PZTN from the amorphous gel to the perovskite structure (Fig. 1.5), with a limited quantity of pyrochlore phase that disappears upon heating at 500°C. The crystallite size was in the range of 20–30 nm but the particles aggregated into hard agglomerates, which preserve the lamellar structure deriving from the gel polymeric network. The influence of the molar ratio of citrate to nitrate onto chemical composition, phase evolution and morphology of $(Pb_{0.93}La_{0.07})[(Zr_{0.60}Ti_{0.40})]_{0.9825}Nb_{0.0175}O_3$ (PZTLN) powders produced by the sol-gel combustion was investigated [84]. Stable sol was obtained by adding nitric acid as oxidiser at C/N molar ratio varying from the stoichiometric (1.30) to an increasing nitrate excess (0.36 and 0.09). PH of the sol was maintained at 7. The polymeric gels resulting from these sols were pyrolysed by an exothermic reaction which becomes an "explosive" process for C/N = 0.09. According to the velocity of the decomposition reaction, the average size of PZTLN powder decreased with lowering C/N ratio. Thus, the powder with the lower C/N ratio presented a uniform microstructure with grain size of about 50 nm diameter bonded in chains and randomly oriented.

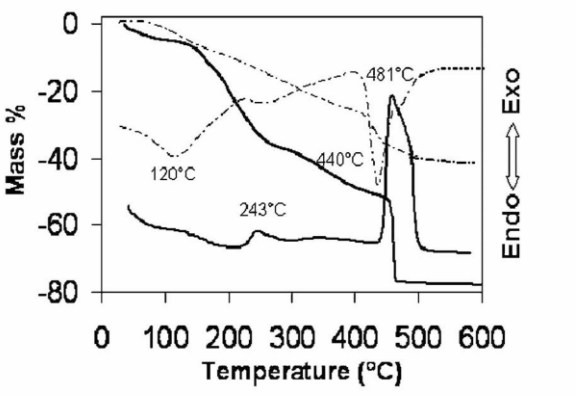

Fig. 1.4 Thermal analysis plots of gel and mixed metal nitrates solution (dot line) (composition PZTN). DTA and TGA analysis of the citrate gel is compared with that of a Pb, Zr, Ti, Nb nitrate mixture prepared by spray-drying the aqueous solution of salts mixed in the same stoichiometric ratio (from [83]).

A significant lead loss was identified that required an excess amount of lead in the starting lead solution. A residual amount of lead carbonate is found at the sintering temperature. Fine Ba-modified bismuth sodium titanate with composition $0.94[(Bi_{0.5}Na_{0.5})TiO_3]$-$0.06BaTiO_3$ (BNBT) powders were prepared by optimising C/N and the gel firing temperature. Decomposition of the precursors and the direct formation of the pure BNBT perovskitic phase in a single step [85]. The best conditions to obtain the desired phase are (C/N) = 0.2, and a combustion temperature of 500°C. Ball milled powders were densified at temperature 100°C lower than that one used in the conventional mixed oxide route. The addition of urea (urea:metal

cations = 1.4:1) prevents the precipitation of metal-citrate compounds as a consequence of pH variations induced by the evaporation of NH_3. The stoichiometry is maintained from gel formation to the sintered body.

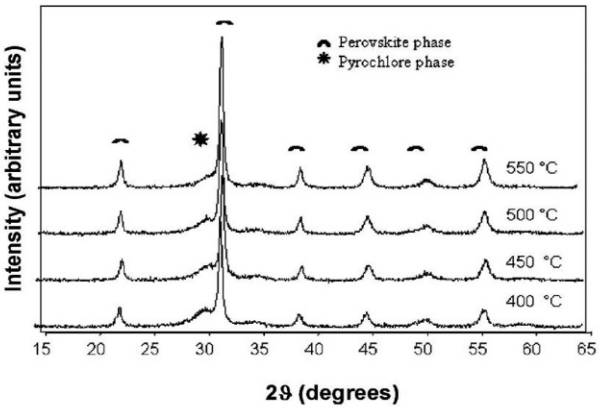

Fig. 1.5 XRD spectra of gel combusted powders calcined at different temperatures (composition PZTN) (from [83]).

1.3.3.4 Direct Synthesis from Solution

In the direct synthesis from solution (DSS) methods, the precipitation of components, consequent to the solvent evaporation, takes place inside the droplets. This ensures a control of stoichiometry at this level. Together with a better control of stoichiometry, DSS methods produce finer particles ensuring a better powder sinterability. In spray-pyrolysis, an aerosol of the precursor solution is directly pyrolised inside the reaction chamber [86]. The aerosol is generated by nozzle atomisation or by ultrasonic atomisation. In the nozzle atomisation, the droplet sizes are relatively large, giving particle sizes of tens of microns. Ultrasonic atomisation is capable of producing aerosols with much smaller droplet sizes, but is generally a low-throughput process.

Recently, $BaTiO_3$ nanoparticles with tunable size (from about 23 to 71 nm) were successfully prepared by flame-assisted spray pyrolysis (FASP) [87]. This was from an aqueous solution of barium acetate and titanium-tetra-isopropoxide, by varying the concentration of precursors and methane flow rate. The flame temperature is a key factor in producing particles with a narrow size distribution. When high methane flow rates are applied, the structure of $BaTiO_3$ nanoparticles is cubic. Hexagonal phase is formed. Nimmo [88] investigated the processing conditions to produce PZT 52/48 powders by twin-fluid nozzle atomisation of

aqueous sol–gel precursor solutions of lead acetate, zirconium acetate, and titanium isopropoxide modified by acetylacetone.

The initial drying and low-temperature decomposition are critical stages for particle morphology. This results in a mixture of spherical and larger collapsed particles with size up to 10 μm. In fact, the rapid solvent evaporation causes surface precipitation as a consequence of solute concentration distribution during the condensation. At reactor temperatures above 800°C, nano-sized elongated particles of lead carbonate are formed on the surface of the PZT particles. The spray drying (SD) is considered a promising method of producing high quality powders for the synthesis of multicomponent systems. The properties of such powders are strongly dependent on chemical homogeneity. In comparison to other solution techniques, the spray-drying process is quite simple. It permits a good theoretical simulation of experimental parameters to optimise the process. PZTN powders can be produced by spray drying [89] the solution of lead and zirconium nitrates, niobium ammonium complex, and titanium isopropilate in a hot air stream. This results in minute spherical granules.

To break up the agglomerates, different milling procedures were tested, including ball milling and ultrasonication. There is a high reactivity of the very fine powder that leads to the formation of the perovskitic phase at 550°C. But the hollow sphere morphology of the agglomerates results in inhomogeneous microstructure even after sintering (Fig. 1.6). The efficiency of the synthesis by spray drying a solution is strongly limited by the maximum concentration of the salts in the precursor solutions. In this case, as the four salts show the maximum solubility in different conditions, the concentration of the multi-component solution is governed by the solubility of lead and zirconium nitrates in nitric acid. The maximum concentration reachable resulted 0.2M on lead basis at pH=1.

By carefully controlling the stoichiometry and the milling procedure, Bezzi [90] obtained a homogeneous material with as good properties as the one produced by the solid state reaction. However, this was at a 100°C lower sintering temperature. PMN powders were prepared [91] starting from an aqueous nitrate solution containing Pb^{2+}, Mg^{2+} and Nb^{5+} cations. On heating at 450°C, the pyrochlore phase is formed. The perovskite phase coexists with pyrochlore and unreacted PbO in the temperature range 700–800°C. They are almost completely transformed into the perovskite phase at 800°C. Above 800°C, the PbO partially evaporates and the pyrochlore phase is formed again. The direct synthesis of the perovskite phase is possible during densification when the amorphous starting powder calcined at 350°C is used. The densification takes place simultaneously to the formation of the perovskite phase, when the samples are sintered at 1050°C through a reaction sintering mechanism.

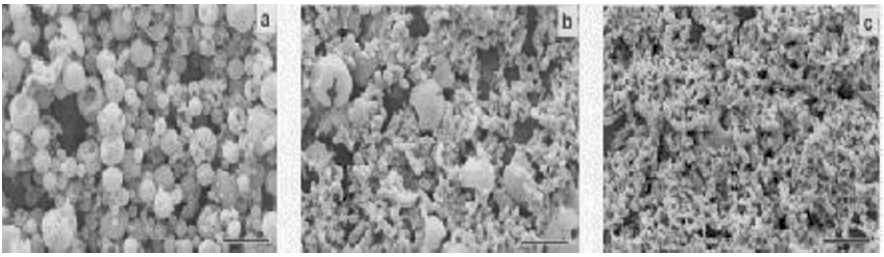

Fig. 1.6 SEM morphology of SD powders: powder As sprayed **a** after ball milling, **b** and after sintering **c**; bar =5 μm (from [89]).

1.3.3.5 Hydrothermal Synthesis

A solvothermal process can be defined "a chemical reaction in a closed system in the presence of a solvent (aqueous and non aqueous solution) at a temperature higher than that of the boiling point of such a solvent" [92]. Consequently, a solvothermal process involves high pressures. Hydrothermal synthesis is a process that utilises single or heterogeneous phase reactions in aqueous media at elevated temperature (T>25°C). Pressure (P>100 kPa) is used to crystallise anhydrous ceramic materials directly from solution [93]. The precursors can be solutions, gels, and suspensions. Inorganic or organic additives are often used at high concentrations to control pH or to promote solubility. Other additives are used to promote particle dispersion or control crystal morphology. For large scale production of materials, typical temperature and pressure fall around 350°C and 100 MPa (saturated vapour pressure of water at this temperature is 16 MPa), while milder or more severe reaction conditions are also considered. A thermodynamic model was developed to determine the formation conditions of the lead titanate zirconate, starting from the thermodynamic data of the solids and aqueous species [94]. This led to the synthesis of phase pure PZT at minimum temperatures (150-200°C) and optimum reagent conditions.

Also adjusted were KOH concentration and the amount of PbO [95], and the size and the morphology of the PZT powder. PZT 52/48 nanocrystals were prepared [96] with morphology changing from particle to rod and wire. For this, the ratio of polyvinyl alcohol to polyacrylic acid used as surfactants and reaction time was adjusted. Nano-sized BT powders have been produced by several low-temperature methods and hundreds of paper have been published. Recently, Wei *et al.* [97] successfully synthesised highly dispersed $BaTiO_3$ nanocrystals of 5–20 nm in size. This was done via a solvothermal method using the mixture of ethylenediamine and ethanolamine as the solvent. Pure perovskite KTN particles have been solvothermally synthesised under a milder condition, such as a lower reaction time and [KOH] in comparison to the hydrothermal route [98]. The sol-gel hydrothermal process was applied to produce NKBT nanowires at T below 200°C [99]. First, a dry gel is prepared by heating at 80°C the sol obtained. A mixture of bismuth nitrate dissolved in acetic acid and potassium and sodium

nitrates dissolved in water is added into the solution of tetrabutyl titanate in ethanol. The gel is suspended in the 10 M solution of NaOH and hydrothermally treated at T 100°–200°C under autogenerated pressure for 48 hours. At 160°C, crystalline nanowire are formed and the NKBT is formed that show upon densification superior properties to that prepared by the conventional sol-gel or solid state reaction.

The conventional hydrothermal method is a time-consuming process that could take several days. It can be enhanced by introducing microwaves into the reaction vessels (microwave hydrothermal process) to reduce synthesis times and temperatures as shown for PZT 52/48 [100].

The influence of microwave frequency, bandwidth sweep time, and processing time on the particle size, phase, microstructure, and porosity of barium titanate prepared by microwave hydrothermal processing has been systematically investigated [101]. These have been compared with results obtained with conventional hydrothermal synthesis (170°C for 2 to 40 hours). The $BaTiO_3$ nanoparticles show global cubic structure with local tetragonal clusters. Increasing the sweep time results in hexagonal phase impurity. This indicates that the transient heating patterns were not uniform, and that the particle growth was slower than for conventional hydrothermal synthesis.

Well crystallised BST nanopowders have been synthesised under supercritical conditions [102] through a single step continuous synthesis over the entire range of composition. This is done in the temperature range of 150°C–380°C at 26 MPa using a continuous process from a mixing of barium, strontium and titanium isopropoxides in ethanol (feed solution) [103]. The synthesis was carried out in an 8 m tubular coiled reactor fitted with an external heater. The first part of the reactor was heated at 150°C and the last one at 380°C.

1.4 Colloidal Processing

1.4.1 Slurry Formulation

Submicrometer-sized (with a tendency towards nano-sized) powders are generally employed in the processing of ferroelectric materials to reduce the densification temperature. This is also to obtain fine grained microstructures with significant improvements in properties. A major problem of fine particles is that they spontaneously agglomerate due to van der Waals attractive forces. This results in inhomogeneous particle packing and pore-size distribution in the green body. The inhomogeneities, being introduced in a larger scale than the primary particles themselves, will control the microstructure evolution during sintering. Therefore, they must be minimised during the cold consolidation treatments. Colloidal processing [104] is a means to address the problem. It prevents the agglomerate formation by

controlling and manipulating the interparticle forces. It eliminates by sedimentation the hard agglomerates formed by partial sintering of primary particles in previous calcining steps [105].

The green body properties are significantly influenced by controlling the state of the powder dispersion (colloidally stable or flocculated). In general terms, colloidally stable suspensions result in more densely packed green bodies with more narrow pore distribution that strongly flocculated suspensions. In contrast, weakly flocculated suspensions have been shown to result in optimal green bodies with some advantages [106]. Many studies have attempted to find the optimal dispersion conditions to maximise the properties of the sintered body. The powders are preferably dispersed in aqueous media. However, one of the problems is the solubility of the powder, which makes the interparticle interaction more complex. The resulting stoichiometry alterations can be detrimental for the final properties of the material. The dissolution of $BaTiO_3$ is favoured in acidified water and accounts for the dependence of the electrokinetic behaviour on the solids concentration [107]. Pb dissolution in aqueous PZT suspensions occurs both in acidic and in strong basic conditions and is influenced for example by the dispersants [108].

Although less environmentally compatible, non-aqueous media are often preferred because the wider choice of organic additives makes easier the optimisation of the formulations for several ceramic fabrication methods. The interparticle interaction can be controlled by introducing electrostatic or steric repulsion or a combination of the two. By adding electrolytes, short chain polymers or polyelectrolytes, long or short range repulsive interaction arises, which results in stable or weakly flocculated suspensions. Nano-sized $BaTiO_3$ powder suspensions in decane were cold consolidated by pressure casting and sintered. The final microstructure can be correlated with the dispersion state. The stable or weakly flocculated ones result in good sinterability and better microstructure than those strongly flocculated [109].

The colloidal processing of PZT powder added with Nb_2O_5 in different organic dispersants like toluene, heptane or methyl ethyl ketone (MEK) resulted in high green and sintered densities. This was when suspensions stabilised by electrosteric hindrance [110] were used. The study of the electrokinetic and rheological behaviour of aqueous PLZT suspensions showed the dependence on pH and amount of ammonium polymethacrylate dispersant. However, lot-to-lot variations, the order of dispersant addition, and pH adjustment [111] also influenced the outcome. Polyacrilic acid (PAA) is a good dispersant for many ceramic powders in water, including $BaTiO_3$ [112].

Green bodies of 62% theoretical density can be achieved by slip casting at high pH and very high PAA coverage. Nevertheless, PAA exhibits both passivation and sequestration effects at the $BaTiO_3$ solution interface [113]. Sequestering occurs at pH>8 and Ba^{2+} dissolution increases linearly with PAA concentration, while a relatively strong passivation was found for PAA in acidic solution. Recently, Yoshikawa *et al.* [114] showed that comb polymer architectures like poly methacrylic acid) (PMAA), are less dependent on ionic strength in comparison to the pure polyelectrolyte. This was when they were used as a backbone, combined with poly

ethilene oxide (PEO) as a charge neutral teeth. Upon increasing the molecular weight of the teeth, they are less susceptible to conformational changes induced by counter-ions in the dispersion of $BaTiO_3$ fine particles in water. Further, comb copolymers can associate the binding effect to the dispersing one [115].

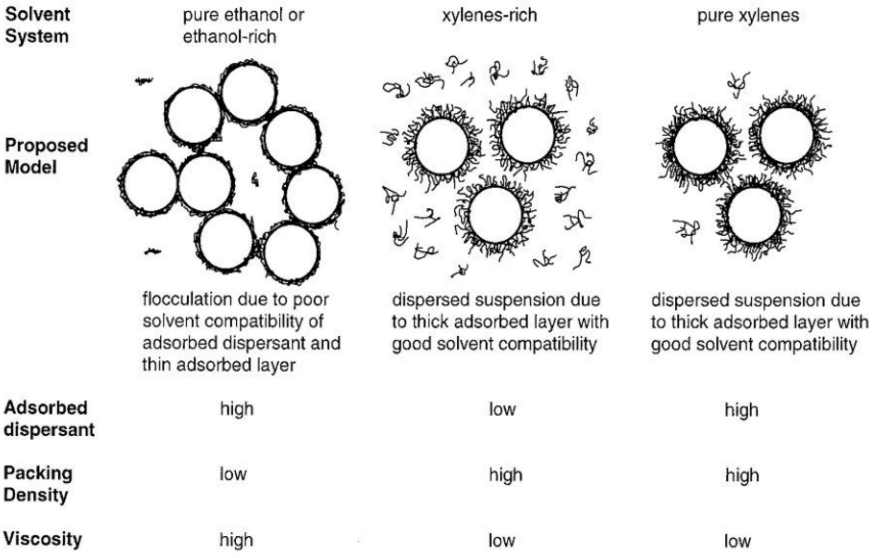

Fig. 1.7 Models for dispersion state of particles in different solvent mixtures containing the same amount of dispersant (from [118]).

1.4.2 Suspension-Based Shaping Techniques

Colloidal processing is the basic approach for the formulation of suspensions for most of the wet cold consolidation routes. This is for routes such as tape casting, screen printing, electrophoretic deposition, ink jet printing, and other direct writing methods.

1.4.2.1 Tape Casting

Tape casting is largely used [116] for the preparation of thin bulk sheets with thickness in the range 50 – 800 μm. These are the basic building blocks in many electro-ceramic components including multilayer ceramic packages. The slurry is deposited on a carrier surface via the doctor blade technique. The coating dries and forms a flexible layer consisting of a polymeric matrix filled with the ceramic

powder [117]. After a debonding treatment to eliminate the organic additives, the material is directly sintered. Traditionally, the suspensions were based on organic solvents due to their low latent heat of evaporation and low surface tension. Binary solvent systems are commonly used because of their increased ability to dissolve the organic additive and faster drying. Often, they are based on ethanol (EtOH) (with methyl-ethyl-ketone, or toluene or xylene), and the mixing ratio can be a critical parameter for the optimisation of the slurry performance (Fig. 1.7) [118]. The dispersant can combine electrostatic or steric effects while binders and plasticisers confer to the tape the necessary flexibility for the further handling. Effective deflocculants in organic medium are glycerol tryoleate and phosphate ester [119]. Polyvinylbutyral, eventually at different molecular weights, is typically used as the binder, combined with butylbenzylphtalate as the plasticiser. Nano-sized PZT powders were dispersed in organic medium [120]. Various ferroelectric materials (BST, PZT, etc.) have been successfully tape cast by adjusting the combination of the same organic components [121]. Then, they were laminated to produce co-fired multimaterial structures with well defined interfaces without delamination.

More critical parameters for successful processing are the ratio between the binder and the plasticiser, the order of the addition of the ingredients, and the milling procedure (that is typically prolonged for 24 hours). Recently, interest has been focused on the production of aqueous suspensions [122] that result in far more sensitive process perturbations. These are drying conditions, casting composition or film thickness, pH, and dissolution of the ceramic powder. Therefore, a careful control of the compositional and process variables is required. Two different types of binders can be selected: water soluble binders (like cellulose ethers, polyvinyl alcohol), or water-emulsion binders (dispersions of non-soluble binder particles in water) like acrylics, vinyls, or polyurethane. The deflocculants are usually polyelectrolytes, as mentioned previously. A wetting agent is often added as the wetting behaviour on the carrier film is a critical issue. The complexity of the variables to be controlled is well represented in the work of Smay *et al.* [123].

Laminated PZT multilayers were produced by tape casting water-based slurry. Aqueous dispersion of nano-sized $BaTiO_3$ dispersed with NH_4-PAA with PVA as the binder, and glycerol as plasticiser, has produced homogeneous green body and 95% rel density upon sintering at 1200°C [124]. Feng *et al.* studied the effect of molecular size and chemical structures of plasticisers and binders (PVA with varying molecular weights and hydrolysis percentages), on the mechanical properties of the green tapes of PLZT powder [125]. During drying, a stress evolution occurs because of constrained volume shrinkage. The latter stage of drying is linked mainly to the polymer phase that undergoes coalescence and affects the residual stresses depending on the polymer chain mobility or on the hydrolysis level of PVA. The higher hydrolysis generates larger stresses in the green tapes. Water-soluble PMAA-b-PEO polyelectrolyte was used to disperse PLZST powder, with PVA as binder and PEG as plasticiser. The green tape resulted in very flexible and almost fully dense sintered body [126]. Deliormanli *et al.* [127] showed that the use of comb polymer PAA-PEO with a non-ionic acrylic latex emulsion, and hy-

droxypropyl methylcellulose and the preparation by a multi-step process, led to high solid loading PMN suspensions. The final microstructure is homogeneous as a consequence of the careful control of the rheological properties and wetting and drying behaviour of the slurry.

1.4.2.2 Electrophoretic Deposition

Electrophoretic deposition (EPD) is usually carried out in a two-electrode cell in two steps [128]. In the first step, an electric field is applied between two electrodes and charged particles suspended in a suitable liquid move toward the oppositely charged electrode (electrophoresis). In the second step, the particles accumulate at the deposition electrode and create a relatively compact and homogeneous film (deposition). Therefore, it is necessary to produce a stable suspension containing charged particles free to move when an electric field is applied. After the deposition, a heat-treatment step is normally needed to further densify the deposit. The technique is mainly applied to produce coatings and films. Thick films of ferroelectric materials have consequently been developed [129, 130]. Moreover, it is of interest to produce monolithic ceramics, ceramic laminates, fibre reinforced composites and functionally graded materials [131]. The powders can be dispersed in organic medium (often ethanol) or water. PH, zeta potential, and conductivity are critical parameters in the control of the deposit homogeneity [132]. Recently, magnetic field-assisted EPD has been applied to obtain grain-oriented $Bi_4Ti_3O_{12}$–$BaBi_4Ti_4O_{15}$ (BiT-BBTi) [133]. The powder dispersed in ethanol with phosphoric ester and polyethylenimine is aligned along a specific crystallographic orientation by applying a magnetic field among the facing electrodes and an electric voltage. The dried compacts were sintered to 97% relative density. It showed that the alignment of the particles induced by the magnetic field in the suspension, remains in the green compacts and is further enhanced by densification followed by grain growth. The piezoelectric properties are significantly improved in comparison to the randomly oriented samples.

1.4.2.3 Inkjet Printing

Inkjet printing is a mean of fabricating 3D ceramics solid structures. It is a near net shape, tool less manufacturing technique, consisting in the deposition of ceramic ink micro-droplets ejected via nozzles to build the successive layers [134]. Drop-on demand printers are frequently used and very fluid inks are required that rapidly solidify by evaporation of the carrier vehicle (EtOH or MEK/EtOH). Sometimes, the jetting is done at high temperature. PZT parts were fabricated by Noguera *et al.* [135] with a printing head by adjusting the fluid properties of the ceramic suspension (size distribution in relation to the aperture of the nozzle, organic fraction composition – in order to avoid sedimentation) and control drying, viscosity and surface tension. They also controlled the velocity, initial size and

path of the droplets before spreading. Ceramic pillar arrays were fabricated with pillar diameter 110 μm starting from a 10 volume percentage suspension. Minimising the dimensional change between the printed part and the sintered part requires high solid loading suspensions. Only a limited range of viscosity (10-50 mPas) is compatible with this technology. One variant of inkjet printing is phase change or hot melt printing that makes use of a particulate suspension in a low melting point vehicle. The printing occurs at a temperature above its melting point. PZT powder was dispersed by ball milling at 110°C at 40 volume percentage in paraffin wax (melting point 57°C) added with paraffin oil, to lower the viscosity, with a combination of stearylamine and polyester [136]. The parts were printed at the same temperature with a nozzle of 70 μm diameter. The debonding is a critical and time consuming step. The wax is removed by capillary action, by keeping the samples in a powder bed for two days, instead of burning the residual wax by a controlled heating followed by sintering.

1.4.2.4 Electro-hydrodynamic Deposition

Electro-hydrodynamic deposition is an alternative method to downsize the structure, for example for preparing micrometer and sub-micrometer scale composites. It is a method of liquid atomisation. By means of electrical forces, the liquid flowing out of a capillary nozzle, which is maintained at high electric potential, is forced by the electric field to be dispersed into fine droplets [137]. The droplet size can range from hundreds micrometer to tens of nanometer and can be nearly monodisperse. They are electrically charged and are driven by means of an electric field. Electrospray is mostly used for micro- and nano-thin film deposition, micro- or nano-particle production, and micro- or nano-capsule formation. PZT columnar structures have been grown as thick as 35 μm from the 0.6 M sol in 1-propanol and glacial acetic acid, deposited at flow rate 2.5×10^{-11} $m^3 s^{-1}$ and applied voltage 4.2 kV [138].

1.5 Templated Grain Growth

Microstructure control is a key issue in optimising the performance of the ferroelectric materials. Microstructure evolution has been extensively investigated. The sintering process involves both densification and grain growth. The densification process is the replacement of solid and vapour interfaces either by solid and solid interfaces (solid-state sintering), or by solid and liquid interfaces (liquid phase sintering). Grain growth is related to the minimisation of total interfacial area by interface migration. The driving force and kinetics of sintering are related to interfacial energy evolution. Capillarity effect drives grain coarsening or Ostwald ripening of solid grains dispersed in a liquid matrix. Grains smaller than average dissolve and larger ones grow. In the solution-reprecipitation process, surface struc-

ture strongly affects the growth of the new grains. Pore and grain size are closely related because of geometrical constraints that impose a critical pore to size ratio above which the pore is stable. In most ferroelectric materials, a liquid phase is present during densification, at least as a thin intergranular film. Grain growth occurs by the migration of the solid-liquid interface. Sintering in oxygen is a further key step in obtaining fully dense ferroelectrics. Pores filled with oxygen can close more easily due to the faster diffusion of oxygen in comparison to the slower diffusion of nitrogen that is the major component of air.

The crystallographic texturing of polycrystalline ferroelectric ceramics has been intensively investigated since the finding by Park and Shrout [139] that relaxor-based ferroelectric single crystals show remarkably higher piezoelectric strains than ceramics, primarily in the (001) crystal orientation. Similar increased properties have been found even in $BaTiO_3$ and Zr-doped $BaTiO_3$. The efforts to produce single crystals have resulted in a significant progress in the production of larger single crystals. But the difficulties in controlling the uniformity of the concentration, particularly for MPB crystals, and the intrinsically high costs still limit the diffusion of the single crystal technology. Therefore, the scientific and commercial interest in the processing and properties of textured ceramics has increased significantly. Templated Grain Growth (TGG) consists of the nucleation and growth of the desired polycrystalline material on aligned single crystal template particles. This results in an increased fraction of oriented material upon heating. The template particles must be anisometric, to promote the alignment during cold consolidation. Single crystals must act as preferred growth sites and chemically stable up to the densification temperature. In a reactive matrix they can be the seed sites for the phase formation (Reactive Templated Grain Growth RTGG) [140].

In a comprehensive review, Messing *et al.* [141] showed that more than one to more than three times higher d_{33} values are obtained for all the compositions investigated. Texturing degree as high as 90% can be obtained. TGG can be homoepitaxial when the growing single crystal has the same composition and crystal structure of the template material. It can be heteroepitaxial when the template has a different composition but the same crystal structure, or when there is matching between the lattice and the matrix. A small amount of larger template particles is dispersed in a finer and equiaxed particles matrix. It is subsequently oriented, usually by shear forming processes like tape casting or extrusion. Anisometric particles can be induced to align under a gated doctor blade. During densification, once the ceramic exceeds 95% density, texture evolves by growth of the template particle. They can act as nucleation sites and seed the phase transformation of the matrix [142].

The growth process is sustained by a size ratio between the template particles and the matrix grains larger than approximately 1.5. It is often enhanced by a liquid phase. The template particles must have similar crystal structure and less than 15% lattice parameter mismatch with the phase to be templated. High aspect ratio with axis matching the crystallographic expectation is preferable, like stability in the presence of the liquid phase at the growth temperature. Therefore, the most preferred are whisker or platelet shaped particles with a small grain size that after

growth should not exceed the mean size of 40 µm. They are produced by molten flux or hydrothermal synthesis [143,144]. Perovskites like $PbTiO_3$, $BaTiO_3$, and $SrTiO_3$ are used as templates for complex peroskitic systems like PMN-based relaxors, because of the small lattice mismatch. Brosnan *et al.* recently used tabular $SrTiO_3$ [145] to optimise the processing conditions for highly textured PMN-28PT composition. 20 µm thick green tapes were stacked to 60-70 layers, laminated, debonded and isostatically pressed to about 54% TD. After sintering at 1150°C, (15 hours soaking) in lead atmosphere and flowing oxygen, an almost fully dense material was obtained with templated grains with average size of 40 µm. No residual $SrTiO_3$ grains were found as they were rather fine. A soaking at 750°C was necessary to stabilise the templates against dissolution in the PbO rich intergranular phase before the beginning of the TGG process. An increase of the piezo coefficient by a factor of up to 1.8 was found [146] by templating PMN-32PT and PMN-37PT-21PZ materials with $BaTiO_3$ platelets, following similar processing conditions. Plate-like $NaNbO_3$ was used as reactive template to texture compositions in the system $(KNa)NbO_3$-$LiTaO_3$ [147] by RTGG method. This led to obtaining a Lotgering factor of orientation higher than 90% and excellent piezoelectric properties. The $NaNbO_3$ particles were synthesised by a topochemical reaction in which the particle morphology was preserved and a <001> plane of the perovskite was developed by ion exchanging the Na for Bi ions on bismuth layer-structured plate-like composition. Recently, materials in the BNT and BNBT system were textured with templates of the composition $Bi_4Ti_3O_{12}$ (BiT) by TGG [148], and through RTGG by varying the Na content from 2 mol% excess to 2 mol% deficient [149].

The evolution of the microstructure of the sample with Na -excess shows texturing already at temperature lower than 800°C. This was attributed to the formation of a liquid phase (that promotes the dissolution of the polycrystalline matrix grains and deposition on the lowest energy surface that is the single crystal template). A large degree of orientation remains at the densification temperature, but some porosity remains in the final microstructure (final density about 93%). Gao *et al.* [150] measured the piezoelectric properties of NKBT textured with BiT template particles, in the perpendicular and parallel to the tape casting direction. He found a significant improvement in comparison to the conventional process.

1.6 Conclusions

In recent years, the research on the processing of ferroelectric materials has been extended to new compositions and routes to produce powders with controlled morphology, mostly reduced size, and controlled size distribution towards the nano scale. Some of the most investigated processes to produce fine powders were reviewed in the present work, together with a few of the processing routes to produce cold consolidated bodies. Control of the powder agglomeration is a critical issue both during the powder synthesis and in the shaping step. Wet forming

methods are widely used to control the green body homogeneity. Further, templated grain growth has been focused as a means to enhance the properties of new lead-free materials.

References

1. Jaffe B, Cook WR and and Jaffe H (1971) Piezoelectric Ceramics Academic Press, London and New York
2. Rabe KA, Dawber M, Lichtensteiger C, Ahn CH and Triscone JM (2007) Modern physics of ferroelectrics: Essential background Physics of Ferroelectrics: a Modern Perspective (Topics in Applied Physics), pp 1-30
3. Haertling GH (1999) Ferroelectric ceramics: History and technology, Journal of the American Ceramic Society 82: 797-818
4. Bhalla AS, Guo RY and Roy R (2000) The perovskite structure – a review of its role in ceramic science and technology. Materials Research Innovations 4: 3-26
5. Lee T and Aksay IA (2001) Hierarchical structure-ferroelectricity relationships of barium titanate particles. Crystal Growth & Design 1: 401-419
6. Lee S, Randall CA and Liu ZK (2007) Modified phase diagram for the barium oxide-titanium dioxide system for the ferroelectric barium titanate. Journal of the American Ceramic Society 90: 2589-2594
7. Markovic S, Mitric M, Cvjeticanin N and Uskokovic D (2006) Structural and dielectric properties of $BaTi_{1-x}Sn_xO_3$ ceramics In: Uskokovic DPMSKRDI (ed), pp 241-246
8. Jaffe B, Roth RS and Marzullo S (1954) Piezoelectric properties of lead zirconate-lead titanate solid-solution ceramics. Journal of Applied Physics 25: 809
9. Kakegawa K, Mohri J, Takahashi T, Yamamura H and Shirasaki S (1977) Compositional fluctuation and properties of $Pb(Zr,Ti)O_3$. Solid State Communications 24: 769-772
10. Cao WW and Cross LE (1993) Theoretical-model for the morphotropic phase-boundary in lead zirconate lead titanate solid-solution. Physical Review B 47: 4825-4830
11. Noheda B, Cox DE, Shirane G, Gonzalo JA, Cross LE and Park SE (1999) A monoclinic ferroelectric phase in the $Pb(Zr_{1-x}Ti_x)O_3$ solid solution. Applied Physics Letters 74: 2059-2061
12. Cordero F, Craciun F and Galassi C (2007) Low-temperature phase transformations of $PbZr_{1-x}Ti_xO_3$ in the morphotropic phase-boundary region. Physical Review Letters 98255701
13. Bokov AA and Ye ZG (2006) Recent progress in relaxor ferroelectrics with perovskite structure. Journal of Materials Science 41: 31-52
14. Shrout TR and Zhang SJ (2007) Lead-free piezoelectric ceramics: Alternatives for PZT? Journal of Electroceramics 19: 111-124
15. Maeder MD, Damjanovic D and Setter N (2004) Lead free piezoelectric materials. Journal of Electroceramics 13: 385
16. Mehring M (2007) From molecules to bismuth oxide-based materials: Potential homo- and heterometallic precursors and model compounds. Coordination Chemistry Reviews 251: 974-1006
17. Baettig P, Schelle CF, LeSar R, Waghmare UV and Spaldin NA (2005) Theoretical prediction of new high-performance lead-free piezoelectrics. Chemistry of Materials 17: 1376-1380

18. Takenaka T, Maruyama K and Sakata K (1991) $(Bi_{1/2}Na_{1/2})TiO_3$-$BaTiO_3$ system for lead-free piezoelectric ceramics. Japanese Journal of Applied Physics Part 1-Regular Papers Short Notes & Review Papers 30: 2236-2239
19. Nagata H, Yoshida M, Makiuchi Y and Takenaka T (2003) Large piezoelectric constant and high Curie temperature of lead-free piezoelectric ceramic ternary system based on bismuth sodium titanate-bismuth potassium titanate-barium titanate near the morphotropic phase boundary. Japanese Journal of Applied Physics Part 1-Regular Papers Short Notes & Review Papers 42: 7401-7403
20. Isupov VA (2006) Systematization of Aurivillius-type layered oxides. Inorganic Materials 42: 1094-1098
21. Shulman HS, Testorf M, Damjanovic D and Setter N (1996) Microstructure, electrical conductivity, and piezoelectric properties of bismuth titanate. Journal of the American Ceramic Society 79: 3124-3128
22. Maeder MD, Damjanovic D, Voisard C and Setter N (2002) Piezoelectric properties of $SrBi_4Ti_4O_{15}$ ferroelectric ceramics. Journal of Materials Research 17: 1376-1384
23. Wang CM and Wang JF (2008) Aurivillius phase potassium bismuth titanate: $K_{0.5}Bi_{4.5}Ti_4O_{15}$. Journal of the American Ceramic Society 91: 918-923
24. Sanson A and Whatmore RW (2005) Phase diagram of the $Bi_4Ti_3O_{12}$-$BaTiO_3$-$(Na_{1/2}Bi_{1/2})TiO_3$ system. Journal of the American Ceramic Society 88: 3147-3153
25. Jamieson P.B., Abrahams S.C. and Bernstein J.L. (1968) Ferroelectric tungsten bronze – type crystal structures. I. Barium Strontium Niobate $Ba_{0.27}Sr_{0.75}Nb_2O_{5.78}$. The Journal of Chemical Physics 48: 5048-5067
26. Venet M, Vendramini A, Garcia D, Eiras JA and Guerrero F (2006) Tailoring of the lead metaniobate ceramic processing. Journal of the American Ceramic Society 89: 2399-2404
27. Weller MT, Hughes RW, Rooke J, Knee CS and Reading J (2004) The pyrochlore family – a potential panacea for the frustrated perovskite chemist. Dalton Transactions: 3032-3041
28. Ang C and Yu Z (2004) Phase-transition temperature and character of $Cd_2Nb_2O_7$. Physical Review B 70134103
29. Fischer M, Malcherek T, Bismayer U, Blaha P and Schwarz K (2008) Structure and stability of $Cd_2Nb_2O_7$ and $Cd_2Ta_2O_7$ explored by ab initio calculations. Physical Review B 78014108
30. Eerenstein W, Mathur ND and Scott JF (2006) Multiferroic and magnetoelectric materials. Nature 442: 759-765
31. Liu XH, Xu Z, Wei XY and Yao X (2008) Ferroelectric and Ferromagnetic Properties of $0.7BiFe_{1-x}Cr_xO_3$–$0.3BaTiO_3$ Solid Solutions. Journal of the American Ceramic Society 91: 3731-3734
32. Nan CW, Bichurin MI, Dong SX, Viehland D and Srinivasan G (2008) Multiferroic magnetoelectric composites: Historical perspective, status, and future directions. Journal of Applied Physics 103031101
33. Testino A, Mitoseriu L, Buscaglia V, Buscaglia MT, Pallecchi I, Albuquerque AS, Calzona V, Marre D, Siri AS and Nanni P (2006) Preparation of multiferroic composites of $BaTiO_3$-$Ni_{0.5}Zn_{0.5}Fe_2O_4$ ceramics. Journal of the European Ceramic Society 26: 3031-3036
34. Duong GV and Groessinger R (2007) Effect of preparation conditions on magnetoelectric properties of $CoFe_2O_4$-$BaTiO_3$ magnetoelectric composites, pp E624-E627
35. Babu SN, Srinivas K, Suryanarayana SV and Bhimasankaram T (2008) Magnetoelectric properties in NCMF/PZT particulate and bulk laminate composites. Journal of Physics D-Applied Physics 41165407
36. Amin A, Spears MA and Kulwicki BM (1983) Reaction of anatase and rutile with barium carbonate. Journal of the American Ceramic Society 66: 733-738

37. Beauger A, Mutin JC and Niepce JC (1983) Synthesis reaction of metatitanate $BaTiO_{3.2}$. Study of solid-solid reaction interfaces. Journal of Materials Science 18: 3543-3550
38. Yanagawa R, Senna M, Ando C, Chazono H and Kishi H (2007) Preparation of 200 nm $BaTiO_3$ particles with their tetragonality 1.010 via a solid-state reaction preceded by agglomeration-free mechanical activation. Journal of the American Ceramic Society 90: 809-814
39. Buscaglia MT, Bassoli M and Buscaglia V (2008) Solid-state synthesis of nanocrystalline $BaTiO_3$: Reaction kinetics and powder properties. Journal of the American Ceramic Society 91: 2862-2869
40. Buscaglia MT, Buscaglia V, Viviani M, Dondero G, Rohrig S, Rudiger A and Nanni P (2008) Ferroelectric hollow particles obtained by solid-state reaction. Nanotechnology 19225602
41. Lemanov VV (2007) Barium titanate-based solid solutions. Ferroelectrics 354: 69-76
42. Huang CC and Cann DP (2008) Phase transitions and dielectric properties in $Bi(Zn_{1/2}Ti_{1/2})O_3$-$BaTiO_3$ perovskite solid solutions. Journal of Applied Physics 104024117
43. Lee S and Randall CA (2008) A modified Vegard's law for multisite occupancy of Ca in Ca in $BaTiO_3$-$CaTiO_3$ solid solutions. Applied Physics Letters 92, 111904, 1-3
44. Maso N, Beltran H, Cordoncillo E, Sinclair DC and West AR (2008) Polymorphism and dielectric properties of b-doped $BaTiO_3$. Journal of the American Ceramic Society 91: 144-150
45. Chandratreya SS, Fulrath RM and Pask JA (1981) Reaction Mechanisms in the Formation of PZT Solid Solutions. Journal of the American Ceramic Society 64: 422-425
46. Nakamura Y, Chandratreya SS and Fulrath RM (1980) Expansion During the Reaction Sintering of PZT. Ceramurgia international 6: 57-60
47. Shrout TR, Papet P, Kim S and Lee GS (1990) Conventionally prepared submicrometer lead-based perovskite powders by reactive calcination. Journal of the American Ceramic Society 73: 1862-1867
48. Isupov VA (1980) Reasons for Discrepancies Relating to the Range of Coexistence of Phases in Lead Zirconate-Titanate Solid Solutions. Soviet Physics, Solid State (English translation of Fizika Tverdogo Tela) 22: 98
49. Kingon AI, Terblanche PJ and Clark JB (1982) Effect of Reactant Dispersion on Formation of PZT Solid Solutions. Ceramics International 8: 108-144
50. Hiremath BV, Kingon AI and Biggers JV (1983)Reaction sequence in the formation of lead zirconate-lead titanate solid-solution – role of raw-materials. Journal of the American Ceramic Society 66: 790-793
51. Galassi C, Roncari E, Capiani C and Costa A (2000) Influence of processing parameters on the properties of PZT materials In: Galassi C, Dinescu M, Ukino K and Sayer M (eds) Piezoelectric materials: advances in science, technology and applications. Kluwer Academic Publishers, pp 75-86
52. Medvecky L, Kmecova M and Saksl K (2007) Study of $PbZr_{0.53}Ti_{0.47}O_3$ solid solution formation by interaction of perovskite phases. Journal of the European Ceramic Society 27: 2031-2037
53. Shrout TR, Papet P, Kim S and Lee G-S (1990) Conventionally prepared submicrometer lead-based perovskite powders by reactive calcination. Journal of the American Ceramic Society 73: 1862-1867
54. Amer AM, Ibrahim SA, Ramadan RM and Ahmed MS (2005) Reactive calcination derived PZT ceramics. Journal of Electroceramics 14: 273-281
55. Randall CA, Kim N, Kucera J-P, Cao W and Shrout TR (1998) Intrinsic and extrinsic size effects in fine-grained morphotropic-phase- boundary lead zirconate titanate ceramics. Journal of the American Ceramic Society 81: 677-688

56. Galassi C, Roncari E, Capiani C and Craciun F (1999) Processing and characterization of high Qm ferroelectric ceramics. Journal of the European Ceramic Society 19: 1237
57. Swartz SL and Shrout TR (1982) Fabrication of perovskite lead magnesium niobate. Materials Research Bulletin 17: 1245-1250
58. Kwon S, Sabolsky EM and Messing GL (2001) Low-temperature reactive sintering of 0.65PMN – 0.35PT. Journal of the American Ceramic Society 84: 648-650
59. Sutton WH (1989) Microwave processing of ceramic materials. American Ceramic Society Bulletin 68: 376-386
60. Rao KJ, Vaidhyanathan B, Ganguli M and Ramakrishnan PA (1999) Synthesis of inorganic solids using microwaves. Chemistry of Materials 11: 882-895
61. Gabriel C, Gabriel S, Grant EH, Halstead BSJ and Mingos DMP (1998) Dielectric parameters relevant to microwave dielectric heating. Chemical Society Reviews 27: 213-223
62. Vaidhyanathan B, Singh AP, Agrawal DK, Shrout TR, Roy R and Ganguly S (2001) Microwave Effects in Lead Zirconium Titanate Synthesis: Enhanced Kinetics and Changed Mechanisms. Journal of the American Ceramic Society 84: 1197-1202
63. Kong LB, Zhang TS, Ma J and Boey F (2008) Progress in synthesis of ferroelectric ceramic materials via high-energy mechanochemical technique. Progress in Materials Science 53: 207-322
64. Beitollahi A and Moravej M (2004) Phase formation study of PZT nanopowder by mechanical activation method at various conditions. Journal of Materials Science 39: 5201
65. Rojac T, Kosec A, Malic B and Holc J (2006) The application of a milling map in the mechanochemical synthesis of ceramic oxides. Journal of the European Ceramic Society 26: 3711-3716
66. Xue J, Wan D, Lee SE and Wang J (1999) Mechanochemical synthesis of lead zirconate titanate from mixed oxides. Journal of the American Ceramic Society 82: 1687-1692
67. Lee SE, Xue JM, Wan DM and Wang J (1999) Effects of mechanical activation on the sintering and dielectric properties of oxide-derived PZT. Acta Materialia 47: 2633-2639
68. Alguero M, Moure A, Pardo L, Holc J and Kosec M (2006) Processing by mechano synthesis and properties of piezoelectric $Pb(Mg_{1/3}Nb_{2/3})O_3$-$PbTiO_3$ with different compositions. Acta Materialia 54: 501-511
69. Moure A, Pardo L, Alemany C, Millan P and Castro A (2001) Piezoelectric ceramics based on Bi_3TiNbO_9 from mechano chemically activated precursors. Journal of the European Ceramic Society 21: 1399-1402
70. Ferrer P, Alguero M, Iglesias JE and Castro A (2007) Processing and dielectric properties of $Bi_4Sr_{n-3}Ti_nO_{3n+3}$ (n=3, 4 and 5) ceramics obtained from mechanochemically activated precursors. Journal of the European Ceramic Society 27: 3641-3645
71. Villegas M, Moure C, Jurado JR and Duran P (1993) Influence of the calcining temperature on the sintering and properties of PZT ceramics. Journal of Materials Science 28: 3482-3488
72. Calzada ML and Defrutos J (1994) Nonstoichiometric lead titanate ceramics prepared by a wet-chemical processing. Journal of Materials Science-Materials in Electronics 5: 13-16
73. Choy JH, Han YS and Kim JT (1995) Hydroxide coprecipitation route to the piezoelectric oxide $Pb(Er,Ti)O_3$ (PZT). Journal of Materials Chemistry 5: 65-69
74. Junmin X and Wang J (1999) Lead zirconate titanate via reaction sintering of hydroxide precursors. Journal of Materials Research 14: 1503-1509
75. Chen M, Yao X and Zhang L (2001) Preparation of (Pb, La)(Zr, Sn, Ti)O_3 antiferroelectric ceramics using colloidal processing and the field induced strain properties. Journal of the European Ceramic Society 21: 1159

76. Camargo ER, Frantti J and Kakihana M (2001) Low-temperature chemical synthesis of lead zirconate titanate (PZT) powders free from halides and organics. Journal of Materials Chemistry 11: 1875-1879
77. Roy S, Bysakh S and Subrahmanyam J (2006) Crystallization kinetics of homogeneously precipitated lead zirconate titanate using urea: Comparison with the conventional ammonia precipitated sample. Journal of Materials Research 21: 856-863
78. Cernea M, Manea A, Piazza D, Galassi C and Vasile E (2007) Ba $(Ti_{1-x}Sn_x)O_3$ (x=0.13) dielectric ceramics prepared by coprecipitation. Journal of the American Ceramic Society 90: 1728-1732
79. Narendar Y and Messing GL (1997) Kinetic analysis of combustion synthesis of lead magnesium niobate from metal carboxylate gels, Journal of the American Ceramic Society 80: 915-924
80. Sengupta SS, Ma L, Adler DL and Payne DA (1995) Extended x-ray-absorption fine-structure determination of local-structure in sol-gel-derived lead titanate, lead zirconate, and lead-zirconate-titanate. Journal of Materials Research 10: 1345-1348
81. Fumo DA, Jurado JR, Segadaes AM and Frade JR (1997) Combustion synthesis of iron-substituted strontium titanate perovskites. Materials Research Bulletin 32: 1459-1470
82. Banerjee A and Bose S (2004) Free-standing lead zirconate titanate nanoparticles: Low-temperature synthesis and densification. Chemistry of Materials 16: 5610-5615
83. Montanari G, Costa AL, Albonetti S and Galassi C (2005) Nb-doped PZT material by sol-gel combustion. Journal of Sol-Gel Science and Technology 36: 203-211
84. Cernea M, Montanari G, Galassi C and Costa AL (2006) Synthesis of la and Nb doped PZT powder by the gel-combustion method. Nanotechnology 17: 1731-1735
85. Mercadelli E, Galassi C, Costa AL, Albonetti S and Sanson A (2008) Sol-gel combustion synthesis of BNBT powders. Journal of Sol-Gel Science and Technology 46: 39-45
86. Messing GL, Zhang SC, Jayanthi GV and Narendar Y (1993) Ceramic powder synthesis by spray pyrolysis. Journal of the American Ceramic Society 76: 2707-2726
87. Purwanto A, Wang WN, Lenggoro IW and Okuyama K (2007) Formation of $BaTiO_3$ nanoparticles from an aqueous precursor by flame-assisted spray pyrolysis. Journal of the European Ceramic Society 27: 4489-4497
88. Nimmo W, Ali NJ, Brydson R, Calvert C and Milne SJ (2005) Particle formation during spray pyrolisis of lead zirconate titanate. Journal of the American Ceramic Society 88: 839-844
89. Galassi C, Roncari E, Capiani C, Fabbri G, Piancastelli A, Silvano F (2002) Spray-Dried PZT from Precursors: Cold Consolidation and Sintering. Journal of Materials Synthesis and Processing 9: 213-221
90. Bezzi F, Costa AL, Piazza D, Ruffini A, Albonetti S and Galassi C (2005) PZT prepared by spray drying: From powder synthesis to electromechanical properties. Journal of the European Ceramic Society 25: 3323-3334
91. Costa AL, Galassi C and Roncari E (2002) Direct synthesis of PMN samples by spray-drying. Journal of the European Ceramic Society 22: 2093-2100
92. Demazeau G (2008) Solvothermal reactions: an original route for the synthesis of novel materials. Journal of Materials Science 43: 2104-2114
93. Riman RE, Suchanek WL and Lencka MM (2002) Hydrothermal crystallization of ceramics. Annales De Chimie-Science Des Materiaux 27: 15-36
94. Lencka M, Anderko A and Riman RE (1995) Hydrothermal precipitation of lead zirconate titanate solid solutions: thermodynamic modelling and experimental synthesis. 78: 2609
95. Ohba Y, Rikitoku T, Tsurumi T and Daimon M (1996) Precipitation of lead zirconate titanate powders under hydrothermal conditions. Journal of the Ceramic Society of Japan 104: 6-10

96. Ren ZH, Xu G, Wei X, Liu Y, Shen G and Han GR (2007) Shape evolution of Pb (Zr,Ti)O_3 nanocrystals under hydrothermal conditions. Journal of the American Ceramic Society 90: 2645-2648
97. Wei X, Xu G, Ren ZH, Wang YG, Shen G and Han GR (2008) Synthesis of highly dispersed barium titanate nanoparticles by a novel solvothermal method. Journal of the American Ceramic Society 91: 315-318
98. Wei N, Zhang DM, Han XY, Yang FX, Zhong ZC and Zheng KY (2007) Synthesis and mechanism of ferroelectric potassium tantalate niobate nanoparticles by the solvothermal and hydrothermal processes. Journal of the American Ceramic Society 90: 1434-1437
99. Hou YD, Hou L, Zhang TT, Zhu MK, Wang H and Yan H (2007) $(Na_{0.8}K_{0.2})_{0.5}Bi_{0.5}TiO_3$ nanowires: Low-temperature sol-gel-hydrothermal synthesis and densification. Journal of the American Ceramic Society 90: 1738-1743
100. Abothu IR, Lin SF, Komarneni S and Li QH (1999) Processing of $Pb(Zr_{0.52}Ti_{0.48})O_3$ (PZT) ceramics from microwave and conventional hydrothermal powders. Materials Research Bulletin 34: 1411-1419
101. Nyutu EK, Chen CH, Dutta PK and Suib SL (2008) Effect of microwave frequency on hydrothermal synthesis of nanocrystalline tetragonal barium titanate. Journal of Physical Chemistry C 112: 9659-9667
102. Aymonier C, Loppinet-Serani A, Reveron H, Garrabos Y and Cansell F (2006) Review of supercritical fluids in inorganic materials science. Journal of Supercritical Fluids 38: 242-251
103. Reveron H, Elissalde C, Aymonier C, Bousquet C, Maglione M and Cansell F (2006) Continuous supercritical synthesis and dielectric behaviour of the whole BST solid solution. Nanotechnology 17: 3527-3532
104. Lewis JA (2000) Colloidal processing of ceramics. Journal of the American Ceramic Society 83: 2341-2359
105. Lange FF (1989) Powder processing science and technology for increased reliability. Journal of the American Ceramic Society 72: 3-15
106. Velamakanni BV, Chang JC, Lange FF and Pearson DS (1990) New method for efficient colloidal particle packing via modulation of repulsive lubricating hydration forces. Langmuir 6: 1323-1325
107. Paik U and Hackley VA (2000) Influence of solids concentration on the isoelectric point of aqueous barium titanate. Journal of the American Ceramic Society 83: 2381-2384
108. Hsu WT, Yu BY and Wei WCJ (2006) Colloidal processing of $Pb(Zr,Ti)O_3$, part I-Pb dissolution. Journal of Ceramic Processing Research 7: 206-210
109. Bergstrom L, Shinozaki K, Tomiyama H and Mizutani N (1997) Colloidal processing of a very fine $BaTiO_3$ powder – Effect of particle interactions on the suspension properties, consolidation, and sintering behavior. Journal of the American Ceramic Society 80: 291-300
110. Meng CH, Wei WCJ, Shieh J and Chen CS (2006) Colloidal processing of $Pb(Zr,Ti)O_3$ targets part II – Effect of $NbO_{2.5}$ additive. Journal of Ceramic Processing Research 7: 281-287
111. Cho JM and Dogan F (2001) Colloidal processing of lead lanthanum zirconate titanate ceramics. Journal of Materials Science 36: 2397-2403
112. Chen ZC, Ring TA and Lemaitre J (1992) Stabilization and processing of aqueous $BaTiO_3$ suspension with polyacrylic-acid. Journal of the American Ceramic Society 75: 3201-3208
113. Paik U, Hackley VA, Lee J and Lee S (2003) Effect of poly(acrylic acid) and poly(vinyl alcohol) on the solubility of colloidal $BaTiO_3$ in an aqueous medium. Journal of Materials Research 18: 1266-1274

114. Yoshikawa J, Lewis JA and Chun B-W (2009) Comb Polymer Architecture, Ionic Strength, and Particle Size Effects on the $BaTiO_3$ Suspension Stability. Journal of the American Ceramic Society 92:S42-S49
115. Chen LP and Hsu KC (2008) Synthesis of an amide/carboxylate copolymer for barium titanate suspensions. I. As a dispersant. Journal of Applied Polymer Science 108: 2077-2084
116. Mistler RE (1990) Tape casting – the basic process for meeting the needs of the electronics industry. American Ceramic Society Bulletin 69: 1022-1026
117. Mistler RE and Twiname ER (2000) Tape Casting: Theory and practice The American ceramic Society, Westerville
118. Feng JH and Dogan F (2000) Effects of solvent mixtures on dispersion of lanthanum-modified lead zirconate titanate tape casting slurries. Journal of the American Ceramic Society 83: 1681-1686
119. Galassi C, Roncari E, Capiani C and Pinasco P (1997) PZT-based Suspensions for Tape Casting. Journal of the European Ceramic Society 17: 367-371
120. Reddy SB, Singh PP, Raghu N and Kumar V (2002) Effect of type of solvent and dispersant on NANO PZT powder dispersion for tape casting slurry. Journal of Materials Science 37: 929-934
121. Jantunen H, Hu T, Uusimaki A and Leppavuori S (2004) Tape casting of ferroelectric, dielectric, piezoelectric and ferromagnetic materials, Journal of the European Ceramic Society 24: 1077-1081
122. Hotza D and Greil P (1995) Aqueous tape casting of ceramic powders. Materials Science and Engineering a-Structural Materials Properties Microstructure and Processing 202: 206-217
123. Smay JE and Lewis JA (2001) Structural and Property Evolution of Aqueous-Based Lead Zirconate Titanate Tape-Cast Layers. Journal of the American Ceramic Society 84: 2495
124. Song YL, Liu XL, Zhang JQ, Zou XY and Chen JF (2005) Rheological properties of nanosized barium titanate prepared by HGRP for aqueous tape casting. Powder Technology 155: 26-32
125. Feng JH and Dogan F (2000) Aqueous processing and mechanical properties of PLZT green tapes. Materials Science and Engineering a-Structural Materials Properties Microstructure and Processing 283: 56-64
126. Zeng YP, Zimmermann A, Zhou LJ and Aldinger F (2004) Tape casting of PLZST tapes via aqueous slurries, Journal of the European Ceramic Society 24: 253-258
127. Sakar-Deliormanli A, Çelik E and Polat M (2009) Preparation of the $Pb(Mg_{1/3}Nb_{2/3})O_3$ films by aqueous tape casting. Journal of the European Ceramic Society 29: 115-123
128. Sarkar P and Nicholson PS (1996) Electrophoretic deposition (EPD): Mechanisms, kinetics, and application to ceramics. Journal of the American Ceramic Society 79: 1987-2002
129. Nagai M, Yamashita K, Umegaki T and Takuma Y (1993) Electrophoretic deposition of ferroelectric barium-titanate thick-films and their dielectric-properties. Journal of the American Ceramic Society 76: 253-255
130. Doungdaw S, Uchikoshi T, Noguchi Y, Eamchotchawalit C and Sakka Y (2005) Electrophoretic deposition of lead zirconate titanate (PZT) powder from ethanol suspension prepared with phosphate ester. Science and Technology of Advanced Materials 6: 927-932
131. Corni I, Ryan MP and Boccaccini AR (2008) Electrophoretic deposition: From traditional ceramics to nanotechnology. Journal of the European Ceramic Society 28: 1353-1367
132. Ma J and Cheng W (2002) Electrophoretic deposition of lead zirconate titanate ceramics. Journal of the American Ceramic Society 85: 1735-1737

133. Suzuki M, Miyayama M, Noguchi Y and Uchikoshi T (2008) Enhanced piezoelectric properties of grain-oriented $Bi_4Ti_3O_{12}$-$BaBi_4Ti_4O_{15}$ ceramics obtained by magnetic-field-assisted electrophoretic deposition method. Journal of Applied Physics 104: 014102-1-6
134. Calvert P (2001) Inkjet printing for materials and devices. Chemistry of Materials 13: 3299-3305
135. Noguera R, Lejeune M and Chartier T (2005) 3D fine scale ceramic components formed by ink-jet prototyping process. Journal of the European Ceramic Society 25: 2055-2059
136. Wang T and Derby B (2005) Ink-jet printing and sintering of PZT. Journal of the American Ceramic Society 88: 2053-2058
137. Jaworek A and Sobczyk AT (2008) Electrospraying route to nanotechnology: An overview. Journal of Electrostatics 66: 197-219
138. Sun D, Rocks SA, Wang D, Edirisinghe MJ and Dorey RA (2008) Novel forming of columnar lead zirconate titanate structures. Journal of the European Ceramic Society 28: 3131-3139
139. Park SE and Shrout TR (1997) Ultrahigh strain and piezoelectric behavior in relaxor based ferroelectric single crystals. Journal of Applied Physics 82: 1804-1811
140. Tani T (1998) Crystalline-oriented piezoelectric bulk ceramics with a perovskite-type structure. Journal of the Korean Physical Society 32: S1217
141. Messing GL, Trolier-McKinstry S, Sabolsky EM, Duran C, Kwon S, Brahmaroutu B, Park P, Yilmaz H, Rehrig PW, Eitel KB, Suvaci E, Seabaugh M and Oh KS (2004) Templated grain growth of textured piezoelectric ceramics. Critical Reviews in Solid State and Materials Sciences 29: 45-96
142. Suvaci E and Messing GL (2000) Critical factors in the templated grain growth of textured reaction-bonded alumina. Journal of the American Ceramic Society 83: 2041-2048
143. Yoon KH, Cho YS and Kang DH (1998) Molten salt synthesis of lead-based relaxors. Journal of Materials Science 33: 2977-2984
144. Mao Y, Park TJ, Zhang F, Zhou H and Wong SS (2007) Environmentally friendly methodologies of nanostructure synthesis. Small 3: 1122-1139
145. Brosnan KH, Poterala SF, Meyer RJ, Misture S and Messing GL (2009) Templated Grain Growth of < 001 > Textured PMN-28PT Using $SrTiO_3$ Templates. Journal of the American Ceramic Society 92 : S133-S139
146. Richter T, Denneler S, Schuh C, Suvaci E and Moos R (2008) Textured PMN-PT and PMN-PZT. Journal of the American Ceramic Society 91: 929-933
147. Saito Y, Takao H, Tani T, Nonoyama T, Takatori K, Homma T, Nagaya T and Nakamura M (2004) Lead-free piezoceramics. Nature 432: 84-87
148. Jones JL, Iverson BJ and Bowman KJ (2007) Texture and anisotropy of polycrystalline piezoelectrics. Journal of the American Ceramic Society 90: 2297-2314
149. Motohashi T and Kimura T (2007) Development of texture in $Bi_{0.5}Na_{0.5}TiO_3$ prepared by reactive-templated grain growth process. Journal of the European Ceramic Society 27: 3633-3636
150. Gao F, Zhang CS, Liu XC, Cheng LH and Tian CS (2007) Microstructure and piezoelectric properties of textured $(Na_{0.84}K_{0.16})_{0.5}Bi_{0.5}TiO_3$ lead-free ceramics. Journal of the European Ceramic Society 27: 3453-3458

Chapter 2
Processing of Ferroelectric Ceramic Thick Films

Marija Kosec, Danjela Kuscer, Janez Holc

2.1 Introduction

The rapid development of the electronics industry has created the need for high-performance, high-reliability, miniaturised electronic components integrated into various electronic devices. Additional requirements, such as the desired size and weight, low cost, low power consumption, and portability, should be considered to make the devices user friendly and widely accessible. Attempts to miniaturise discrete elements have generally failed due to the difficulty in handling and assembly. A lot of waste material and high costs are also involved. In this approach, the ceramic parts are manufactured as a bulk ceramic, followed by a reduction in size by cutting, polishing, etc., to specified dimensions. The final step is the assembling of a thin layer of ceramic with the other components. This top-down approach imposes limits on the minimum dimensions of the manufactured parts. It constrains the geometry of the parts to simple shapes, like discs, plates, rings, cylinders, etc.

The bottom-up approach, where a layer is built on the substrate, has been shown to be an effective way to produce a thick-film component. The paste, consisting of a fine powder mixed with an organic phase, is deposited on a substrate and fired at a high temperature. The obtained layers, with thicknesses from a few to a few tens of micrometres, are the basis for the thick-film component. This technology enables the direct integration of layers onto the substrates. It therefore eliminates the difficulty of handling the thin, bulk ceramic. Thick-film technology was first successfully applied during the Second World War when conductive silver and resistive carbon inks were deposited on a ceramic substrate. This was to miniaturise an electronic part of a mortar's proximity fuse. The invention of the transistor in the late 1940s initiated an intensive development of this technique. This resulted in more reliable and lower-priced electronic

Jožef Stefan Institute, Jamova cesta 39, SI-1000 Ljubljana, Slovenia

components. These subsequently became widely used in everyday products such as radios and televisions.

Nowadays, thick-film technology is well established. The implementation of an extra element in the form of films is a natural development. Ceramic ferroelectric thick-film structures are incorporated in micro-electro-mechanical systems (MEMS). These integrate the mechanical elements and the electronics on a particular substrate. This integration results in the production of miniaturised, high-power and highly sensitive sensors, actuators and transducers.

Ferroelectric thick films are planar structures that generally consist of a substrate, a bottom electrode, a ferroelectric film and a top electrode (Fig. 2.1). The thickness of the ferroelectric layer is typically between 1 and 100 μm.

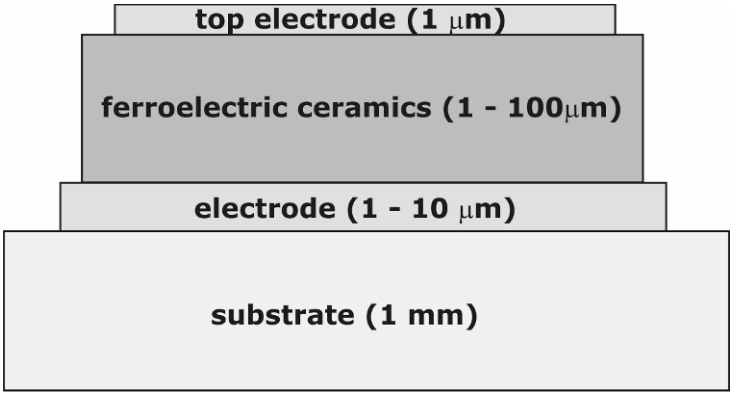

Fig. 2.1. Structure of a ferroelectric thick film.

Ferroelectric thick films are based either on lead-containing or lead-free perovskite materials. The intensive development of ferroelectric materials began in the 1950s with the widespread use of ceramics based on barium titanate ($BaTiO_3$) for capacitors and piezoelectric transducer applications. Later, many lead-based ferroelectric ceramics, including lead titanate ($PbTiO_3$), lead zirconate titanate (PZT), lead lanthanum zirconate titanate (PLZT), and relaxor ferroelectrics such as compositions based on lead magnesium niobate (PMN), were developed and used in a variety of applications. A number of lead-free ferroelectric compositions received attention in the 1990s due to increased environmental awareness. However, only selected compositions have been realised in thick-film form.

Ferroelectric films have been prepared on various substrates like metals (silicon, stainless steel, nickel) and ceramics (alumina, zirconia and, more recently, low-temperature co-fired ceramic (LTCC)). Commonly used electrodes include sputtered or screen-printed metals (platinum, gold, silver, their alloys), oxide-based electrodes (manganites, cobaltites, ruthenates), or composite materials (ruthenate-PZT electrode).

The processing of a thick film involves the synthesis of the powder, the formation of the ink, the deposition of the ink onto the substrate using suitable deposition methods, and the sintering of the deposit to obtain a layer with a good functional response. The processing steps of thick films and bulk ceramics are compared and schematically shown in Fig. 2.2.

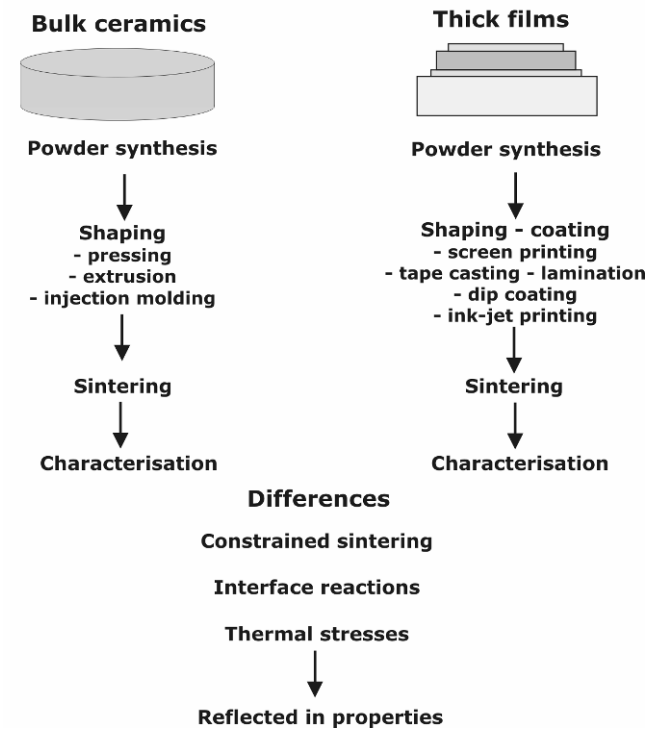

Fig. 2.2. Schematic representation of the processing of thick films as compared to bulk ceramics.

The formation of the thick film involves numerous steps that are characteristic not only for thick films, but also for the manufacturing of bulk ceramics. In both cases, the process begins with the powder synthesis. To obtain a bulk ceramic, the powder-forming processes are chosen on the basis of technical requirements. These include the shape and the size of the product, its microstructure, its properties, its cost, etc. The common forming processes for bulk ceramics include pressing, extrusion, injection moulding and casting. The most common techniques for patterning thick films on various substrates start from powder and include screen printing, pad printing, ink jet, dip coating, electrophoretic deposition, tape casting, and lamination. All these shaping methods require the preparation of suitable suspensions or slurries. After the deposition, the drying and the removal of the organic phases, the green film is fired at a temperature that is sufficient to develop useful properties in the ceramic. In this processing step, referred to as

sintering, the shrinkage of the material occurs. The sintering mechanism in a thick film is different from that in a bulk ceramic. Since ceramic compacts shrink approximately uniformly in the x, y and z directions, the thick films are clamped to the substrate. As a consequence, the film shrinks exclusively in the direction perpendicular to the substrate and is subjected to constrained conditions.

To obtain good functional properties, the ferroelectric layer has to be chemically homogeneous without secondary phases and with a uniform, dense microstructure. The main difficulty with thick-film processing is ensuring good adhesion, avoiding chemical reactions between the layer and the substrate and minimising the sublimation of volatile oxides. To achieve these requirements, lowering the processing temperature is of great interest. Two approaches are commonly used, i.e., to use sub-micron-sized or nano-sized powder and/or to sinter in the presence of a liquid phase. By using fine powder, the densification process can start at a lower temperature [1, 2]. As a result, the reactivity between the thick film's components can be hindered. To increase the density at low temperatures, various compounds with low-melting points are added. However, these additives may reduce the functional response of the layer [3]. It is clear that the densification of the lead-containing perovskite film is improved significantly in the presence of a PbO-based liquid phase [4, 5, 6, 7]. Due to the low melting point, and the high vapour pressure of PbO, it forms a liquid phase that improves the densification process. However, with careful control of the atmosphere during the processing, it can be removed from the film [5].

2.2 Processing of Thick Films

The fabrication of a thick-film is a complex procedure that involves the following basic steps: (1) processing of powders, (2) preparation of suspension, (3) shaping, and (4) densification to produce the desired microstructure of the ceramic.

2.2.1 Processing of the Powder

The starting powder is a crucial factor for processing high-quality ferroelectric thick films. The performance characteristics of a sintered thick film are significantly influenced by the precursor powder's characteristics. Among the most important characteristics are the particle size, the particle size distribution, the chemical composition, and the chemical homogeneity of the powder. Agglomerate-free powders with a narrow size distribution can be compacted with a high green density. When they are in the nano-sized region, these powders can be sintered at reduced temperatures.

A powder that is used for processing a thick film is generally prepared by solid-state synthesis. After the homogenisation, the powder mixture is annealed at

elevated temperatures to ensure the formation of the desired compound. The obtained powder consists of micron-sized particles. Ferroelectric materials have a regularly complex chemical composition, and the processing of a single-phase composition is challenging.

The solid-state processing of perovskite powders with a complex chemical composition may result in a chemically non-homogeneous distribution of the elements in a single-phase calcined powder. One such example is screen-printed $(Pb,La)(Zr,Ti)O_3$ (denoted PLZT) thick films on an alumina substrate [8]. The paste for screen printing was prepared from PLZT powder calcined at 900°C. The chemically inhomogeneous distribution of all the elements was observed after sintering at 1050°C. By increasing the sintering temperature to 1150°C, the chemical homogeneity was generally improved. However, the loss of PbO was observed as a result of the intensified sublimation of the PbO.

One possible approach to processing chemically homogeneous thick films, with complex chemical compositions at temperatures as low as possible, is to use a chemically homogeneous starting powder with nano-sized particles.

Mechano-Chemical Synthesis, also known as high-energy milling, may serve as an alternative to solid-state synthesis. It enables the synthesis of nano-sized powders with a complex chemical composition at close to room temperature by introducing mechanical energy into the powder mixture.

A chemically homogeneous 0.65 $Pb(Mg_{1/3}Nb_{2/3})O_3$ – 0.35 $PbTiO_3$ (denoted PMN-PT) thick film screen printed on a platinised alumina substrate was prepared at 950°C [9, 10]. The suspension was prepared from high-energy-milled powder mixed with an organic phase. The obtained PMN-based powder was characterised by a nano-sized particle and a high chemical homogeneity [11, 12, 13]. PMN-PT thick films were sintered in the presence of a PbO-based liquid phase and this resulted in a single-phase, dense thick film with a good functional response [13]. In addition, by using a low sintering temperature, the chemical reactivity between the thick film and the substrate was minimised.

The Hydrothermal Method is of considerable interest for the synthesis of nano-structured powders and thin- and thick-film layers on metal substrates. This is so because it is a low-cost and environmentally friendly technique. The hydrothermal method utilises the chemical reactions among different ions dissolved in solution and exposed to high temperatures and elevated pressures. Nano-sized PZT powders with spherical particles between 5 and 10 nm have been synthesised from inexpensive metal salts at 160°C [14]. In addition, this method enables not only the synthesis of the compounds from a precursor solution but also a simultaneous deposition on the substrate. A deposit up to a few tens of micrometres thick on a complex shaped substrate can be obtained. PZT- and PMN-based thick films have been grown *in-situ* on a titanium substrate from oxide-based precursors [15, 16, 17, 18].

The Coprecipitation [19, 20, 21] and sol-gel [22] methods have been used for processing ferroelectric thick films from powders.

2.2.2 Shaping Methods

There are a number of suitable methods for making a film in the range of few to a hundreds of μm. These methods can be divided into two groups: those methods primarily designed for thick films (screen printing, tape casting), and those developed for thin films and 3D structures.

2.2.2.1 Screen Printing

The most common method for processing thick films is screen printing. It is a relatively simple process that makes it possible to deposit various materials on a wide variety of substrates, such as ceramics, metals, glass, textile, organic flexible substrates, etc. It is equally well suited to small-scale batches and to high-volume production. This process makes it possible to produce films with thicknesses from a few to several tens of μm with a reliable lateral resolution of above 100 μm.

Screen printing is well suited to the production of electronic components. Its great advantage is its ability to realise the whole structure, ranging from the bottom electrode to the ferroelectric film and the upper electrode, with the same technology and in some cases even with co-firing.

The method requires suspensions with a relatively high viscosity (ink, paste) containing the powder and the "organic vehicle" that is prepared under shear-mode mixing in a three-roll mill. The composition of the suspension should be carefully designed to obtain pseudo-plastic properties in order to moderate the thixotropic properties. In addition, a solvent with a relatively high boiling point is required to avoid drying during the printing. For laboratory experiments the well-known α-terpineol and butylcarbitole are used as the solvents and ethyl-cellulose is used as a binder [23]. The suspension is squeezed through the screen onto the substrate, either manually or automatically. After the deposition, the film is dried to remove the solvents. The desired thickness of the structure is ensured by multiple screen-printing and drying processes. Finally, the organic components, such as polymers and modifiers, are removed from the layer using a thermal treatment between 300°C and 600°C. This is subsequently densified by heating to an appropriate temperature. The technical details of the equipment and the technology can be found elsewhere [3, 24, 25]. The resulting film suffers from a relatively low green density. However, it can be improved by additional isostatic pressing of the green deposit [5, 26].

An adapted screen-printing method was used to prepare PZT films with a thickness up to 3 μm on stainless steel or silicon substrates. To increase the density of the thick film, a sol-infiltration procedure was used [27]. After the screen printing and the burning out of the organic phase, the films were coated with a sol and then sintered [28, 29]. Another process involves the screen-printed and subsequently sintered films being coated with a solution. They are then thermally treated again, but at a lower temperature [30]. After the annealing of

each deposit, the sol was infiltrated into a porous structure and thermally treated [31]. In order to decrease the sintering temperature of the PZT thick films, low-melting point additives were added to the basic dispersed phase [32]. The so-called ComFi technology uses a slurry containing a sol, the powder and low-melting-point additives deposited on a substrate, and the subsequent infiltration of the sol into each deposited layer [1, 33, 34].

2.2.2.2 Tape Casting

Tape casting is a forming technique for producing thin, flat ceramics. The method was originally developed for producing electronic ceramics, including substrates, packages and multilayer capacitors. The tape thickness that can be achieved is generally in the micrometre-to-millimetre range.

The process starts with the preparation of a concentrated suspension containing the deflocculated powder in an organic solvent or water, mixed with several additives, such as dispersing agents, a binder and a softener. The suspension is subsequently cast by means of the tape-casting facility. During the process, the suspension flows from a storage container onto a plastic foil, which is continuously moved with a controlled velocity under the container. A deposit is formed on the plastic foil. The height of this deposit is controlled by a doctor blade, which determines the final thickness of the green tape. After casting the suspension, the green ceramic foil passes into a drying chamber, in which the foil is dried [35].

The green tapes can be used for various applications. They can be laminated and consequently sintered to form ceramic substrates, which have been applicable in thick-film technologies [36, 37, 38]. Lamination is widely used for producing low-temperature, cofired-ceramic (LTCC) tapes. LTCC technology is a three-dimensional ceramic technology utilising the third dimension (z) for the interconnecting layers, the electronic components, and the different 3D structures, such as cantilevers, bridges, diaphragms, channels and cavities. Thick-film technology contributes the lateral and vertical electrical interconnections, and the embedded and surface passive electronic components (resistors, thermistors, inductors, capacitors).

2.2.2.3 Electrophoretic Deposition

Electrophoretic deposition (denoted EPD) is a processing method that enables the shaping of various materials in a variety of shapes and dimensions. For example, it can be used to produce coatings, films, and free-standing objects. EPD is a process in which, in the first step, charged particles, suspended in a liquid medium, migrate towards an electrode when applying an electric field. In the second step, they deposit on an electrode. The suspension for EPD consists of the particles suspended in a solvent with some additives [39].

Aqueous and non-aqueous suspensions can be used for EPD [40]. The solvents should be inert with respect to the powder. The main advantage of aqueous suspensions is that high deposition rates can be obtained by the application of relatively low electric field strengths. However, when applying DC voltages, the electrolysis was found to induce the decomposition of the water and cause gas formation. The deposit may contain pinholes in addition to a lack of adhesion with the substrate. Organic solvents are commonly used for EPD, but they need severe safety precautions, leading to increased processing costs. When compared to other thick-film processing routes, the advantage of EPD is the possibility to process a deposit in a wide range of thicknesses, from a few tens of nanometres to hundreds of millimetres. There is also the possibility to deposit not only on flat but also on curved substrates. In addition, the method is fast, inexpensive, requires simple equipment, and is suitable for mass production.

A comprehensive overview of the electrophoretic deposition of ceramic materials has been published [41]. The PZT deposits were prepared by EPD from water-based suspensions using hydrothermally synthesised PZT powder [42, 43]. It is reported that after sintering at 1100^{o}C, micro-cracks are formed in PZT layers thicker than 5 μm. At this temperature, the PZT chemically interacts with the substrate. A range of non-aqueous colloids have been studied in order to deposit the PZT onto various substrates. PZT films about 20 micrometres thick were prepared from micron-sized PZT powder dispersed in acetyl-acetone with the addition of iodine [44]. PZT particles dispersed in glacial acetic acid have been deposited on an electroded alumina substrate [45], and on metal foils [46, 47]. It is reported that when the sintering occurred in the presence of the liquid phase, by the addition of both Li compounds and PbO, a 10-μm-thick film on Al_2O_3 exhibited a polarisation switching behaviour similar to bulk ceramics. When PZT is deposited on a Cu foil, the formation of a Cu_xPb alloy and, consequently, the deterioration of the functional properties of the PZT thick-film was reported [47]. PZT has been deposited on SiC fibres using a coprecipitated PZT powder suspended in a mixture of water, ethanol, acetone and acetylacetone solvent [19]. High-quality crack-free layers with a thickness up to 40 μm have been reported.

2.2.2.4 Inkjet Printing

Direct-write assembly techniques offer the possibility of fabricating ceramic materials with complex 2D and 3D structures. Inkjet printing involves the direct deposition of colloidal inks in a desired pattern via a layer-by-layer build sequence. The printing information is created directly from a computer and stored digitally. Inkjet printing has several key advantages. It is a simple, non-contact technique that deposits the material in the desired pattern via a nozzle. It avoids the use of screens, printing plates or photolithography. It has good resolution, being capable of depositing tracks with a 50-μm width, with the potential for future improvement. The process is potentially compatible with many rigid and flexible substrates. It enables rapid development and manufacture and is well suited to high-speed,

multilayer processing. It offers the possibility of producing a range of electronic components and three-dimensional structures. It is a low-waste, highly flexible process, equally suited to mass production and small development batches.

The inkjet printing method relies on the formulation of suitable colloidal inks with the desired degree of colloidal stability and rheological behaviour. Colloid inks for direct ink-jet printing typically contain 5 to 40 vol. % of solids. They must be agglomerate-free to avoid clogging of the print-head nozzle and they must form a consistent droplet. This successful droplet formation requires careful control of the surface tension and the rheological parameters of the fluid, such as viscosity, yield stress under shear and compression, and viscoelastic properties. The droplet's spreading influences the lateral resolution and the thickness of the deposit. To minimise it, a high drying rate for the fluid is desired, in addition to the proper surface tension and viscosity.

Numerous successful inkjet printings of PZT have been demonstrated. For example, an aqueous suspension of PZT particles has been successfully deposited on paper [48], and a paraffin-oil/wax-based suspension of PMN–PT has been studied for deposition [49]. A PZT self-standing 3D structure has also been demonstrated [50], and a lot of attention has been given to the inkjet printing of PZT pillar structures, used mainly for ultrasonic transducer applications. The successful fabrication of PZT 1-3 composites has also been demonstrated [51, 52, 53].

2.2.2.5 High Density Deposition Methods

Screen printing, tape casting, inkjet printing, and electrophoretic deposition produce green layers of low density as a result of the low stresses applied to the powder particles during shaping. Deposits with a high density can be obtained by using high energy deposition methods. These techniques rely on the direct deposition of the powder on a certain substrate and are referred to as a jet printing [22, 54], aerosol deposition [55, 56, 57], and airflow deposition [58]. A submicron-sized powder is used, and it is mixed with a high pressure carrier gas to form an aerosol flow. It is then injected into the deposition chamber. The accelerated particles collide with the substrate to form a dense ceramic film at room temperature. These methods enable the low-temperature fabrication of high-quality complex structures, such as mono-morphs, bimorphs, multilayer stacks, and compositionally graded elements [59].

PZT-PMN-based thick films with thicknesses from 5 to 200 μm have been deposited on nickel substrates. A density of ~80 % of the theoretical value (TD) for various thick films has been obtained after the deposition. The green density of aerosol-deposited films is higher than the one obtained for isostatically pressed films, i.e., 67 % TD. After the sintering between 800 and 1000^{o}C, films with more than 98 % of TD and good ferroelectric properties were reported [58]. Lebedev *et al.* [57] reported that a PZT thick film, aerosol deposited on a platinised silicon substrate at 550^{o}C and post-annealed at 600^{o}C, possessed a density higher than 95 % and good functional properties.

2.2.2.6 Thin-Film Adapted Methods

Films with thicknesses of 1 to 10 μm have been prepared using the chemical solution deposition (CSD) method. Two approaches have been used. The first one is multiple spin or dip coating and intermediate firing of the deposit. With this method, PZT films with a thickness of 1 to 4 μm have been prepared on a silicon substrate [60]. It was also reported that 10-μm-thick PZT films prepared by numerous deposition methods exhibited d_{33} values of 220 pm/V. This is comparable to the values of PZT bulk ceramic [61]. Due to the necessity for numerous deposition layers, and the time-consuming processing, the deposition was run automatically. A 15-μm-thick PZT layer has been demonstrated using an automatic dip-coating procedure [62].

The second approach is an adapted thin-film method. The CSD precursor for the coatings is modified with the addition of nano-sized particles with the same composition to increase the solids load in the slurry. Consequently, the viscosity and the density of the slurry are increased. A higher viscosity leads to a thicker deposited layer in a single step. A higher density reduces the subsequent shrinkage and prevents the film from the cracking. When cracks are formed in the deposit, the powder inhibits their propagation. After the deposition process, the film is fired at a typical CSD-processing temperature. This approach is suitable for large-area deposition processes and is compatible with silicon technology.

Deposits with thicknesses of a few tens of micrometers can be processed by the interfacial polymerisation method and a composite precursor. This one-step method used an alkoxide precursor solution that is put into the reaction vessel containing water and the substrate. At the interface of two immiscible liquids, a gel layer is formed. After draining the water, the gel layer is placed on the substrate. After the sintering, a PZT layer with a thickness of 23 μm and a good functional response was obtained [63].

2.2.2.7 Other Methods

Thick films can also be made using micropen writing [64, 65], robocasting [66, 67], the micro-stereo-lithographic process, gelcasting [68, 69], electrohydro-dynamic deposition [70] and others.

2.2.3 Densification of Thick Films

To obtain a suitable functional response, the film has to be chemically homogeneous without an undesirable phase and with a uniform microstructure.

The film deposited on a substrate has to be sintered. The film is clamped to the substrate and therefore it densifies in constrained conditions. In contrast to a bulk ceramic that shrinks isotropically, the thick-film structure shrinks exclusively in

the direction perpendicular to the substrate. This behaviour results in different microstructural characteristics of the film when compared to a bulk ceramic processed under identical sintering conditions (temperature, time, and atmosphere).

During the processing, the thick film is in direct contact with chemically different materials. Therefore, the main difficulty with thick-film processing is ensuring good adhesion as well as avoiding chemical reactions between the film and the substrate. To achieve these requirements, lowering the processing temperature is of great interest. The sintering temperature can be lowered by the addition of low-melting-point compounds or glass frit. This allows sintering in the presence of a liquid phase. The particle size of the powder also influences the sinterability of the thick films. The higher surface/volume ratio of the fine particles consequently leads to a higher density at lower sintering temperatures. By using fine powder, the sintering temperature is lowered. Consequently, the chemical reactivity between the components of the thick-film structure is hindered.

The formation of undesirable reaction products is observed when the layer and the substrate are not chemically compatible phases under particular sintering conditions. The chemical reactivity of the substrate and the thick films may be hindered by incorporating an additional layer between them. This acts as a diffusion barrier that hinders the formation of undesired reaction products. This may therefore improve the adhesion between the film and the substrate.

2.2.3.1 Constrained Sintering

The substrate and the as-deposited layer expand during the thermal treatment of a ceramic thick-film structure deposited on a substrate. At a particular temperature, the film tends to shrink in all directions due to the driving force for sintering. The film is clamped to the rigid substrate and therefore cannot shrink in the plane, but only in the direction perpendicular to the substrate. This results in a tensile stress in the plane of the substrate because the sintering occurs in constrained conditions. The constrained sintering of a thick-film structure on a rigid substrate is schematically shown in Fig. 2.3.

The sintering behaviour of the thick-film structure under constrained sintering conditions has been widely discussed [71, 72, 73]. Under constrained conditions, a slower densification rate and the generation of processing defects have been observed in thick-film structures. This may originate from the stresses that are present in the thick-film structure during the sintering. The in-plane tensile stresses reduce the driving force for sintering and promote the formation of cracks in the structure. The magnitude of the tensile stress depends on the shear rates and the densification rate of the film. When the thick-film structure responds in an appropriate way to the stresses, the number of defects is reduced and the density is improved.

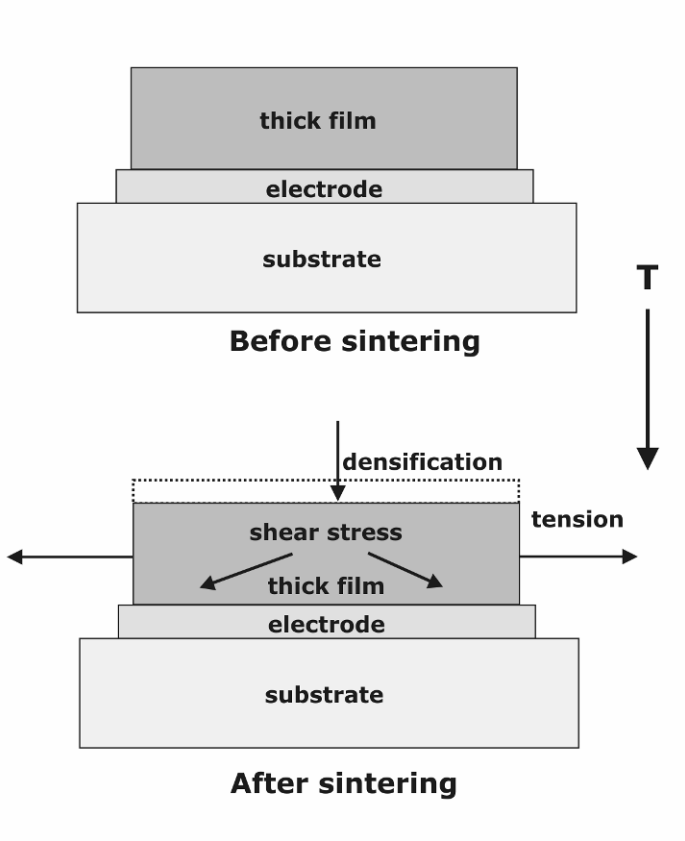

Fig. 2.3. Schematic representation of the constrained sintering of a thick film on a rigid substrate.

The presence of a liquid seems to be beneficial, since it helps release the shear stress through a process of particle rearrangement. This may also be due to enhanced transport via a stress-supported dissolution-precipitation mechanism. The need for a liquid phase to obtain high-density films was confirmed by sintering PLZT thick films [5]. The presence of a liquid phase (PbO based) was ensured by a PbO-saturated atmosphere that prevented the sublimation of the lead oxide, which was initially added to the PLZT in excess [74]. For a comparison, the other samples were kept in an atmosphere that allowed switching from liquid- to solid-phase sintering. The densification was retarded with the disappearance of the liquid phase. The amount of liquid phase can, however, be kept low [5].

The shear stress can be released via particle rearrangement (sliding) and/or enhanced transport processes involving a stress-supported dissolution-precipitation mechanism. This leads to coarsening and reshaping of the grains. The densification of the film is enhanced in comparison with the bulk [5]. Even a minor amount of liquid phase, provided by the capillary condensation of PbO in the pellets with an initially stoichiometric composition, supports densification [75, 76].

2.2.3.2 Sintering in the Presence of a Liquid Phase

The densification of thick-film structures is enhanced in the presence of a liquid phase. Several requirements should be taken into account when designing the sintering in the presence of a liquid phase. First, the melting point of the additive should be lower than the onset sintering temperature of the material. This compound has to be thermodynamically stable in equilibrium with other thick-film components under the processing conditions (temperature, atmosphere). The additive is usually not a ferroelectric material and may reduce the ferroelectric response of the layer. When the additive forms a solid solution with the ferroelectric material, it can change the functional response due to doping. The amount of liquid should be optimised to minimise its influence on the functional properties. It can also be transient and disappear during the processing as a result of evaporation and/or incorporation into the film.

PbO is often used for the processing of lead-based ferroelectric thick films. The addition of a few weight percent of excess PbO to the PZT starting powder gives a corresponding amount of PbO-based liquid phase at temperatures above the melting point of the ternary eutectic in $PbO–ZrO_2–TiO_2$ [77].

PbO liquid-phase-assisted sintering was exploited in several lead-based thick-film structures [5, 6, 7, 13, 78, 79, 80, 81, 82, 83]. Typically, 1 to 5 mol % of PbO is added to lead-based ferroelectric material to ensure sintering in the presence of the liquid phase. However, due to the high vapour pressure of PbO under the sintering conditions, it tends to sublimate from the film. It is necessary, therefore, to ensure a PbO-rich atmosphere around the sample during the sintering course to prevent the loss of PbO from the layer. It is highly desirable that the film does not contain a secondary phase after the sintering. An attempt has been made to remove the PbO-based liquid phase from the film during the final stage of the process.

It was shown that a range of microstructural properties and a very different functional response can be obtained for a 0.65 $Pb(Mg_{1/3}Nb_{2/3})O_3$–0.35 $PbTiO_3$ thick film sintered at an identical temperature and time. This needed a different PbO-atmosphere, determined by the amount of packing powder [13]. When a PMN-PT thick film was surrounded by a small amount of packing powder, all the excess PbO sublimated from the PMN–PT in the initial stage of the sintering. The period when the liquid PbO was present in the PMN–PT was not sufficiently long to obtain a dense PMN–PT layer. The film was then characterised by poor functional properties. When using a larger amount of packing powder around the sample, the excess PbO remained in the PMN–PT for a longer period of the thermal treatment. This resulted in liquid-phase sintering. The film sintered with an optimal amount of packing powder was thinner and denser, with a significantly better functional response. When using a large amount of packing powder, the PbO remained in the sample. Even though the PMN–PT film is dense, its functional response was lower due to the presence of a thin PbO dielectric layer at the grain boundaries of the PMN-PT.

PbO and various compounds or glass frits with a low melting point have been added to the starting powder, to lower the processing temperature of ferroelectric

thick films. For lead-based ferroelectrics, the sintering temperature can be lowered with binary and ternary mixtures of low-melting oxides such as $Pb_5Ge_3O_{11}$ [63, 84, 85], Cu_2O-PbO [1, 32, 33], Li_2CO_3-Bi_2O_3 [86, 87], Bi_2O_3-ZnO [30], Li_2CO_3-Bi_2O_3-CuO [88], $Pb_5Ge_2SiO_{11}$ [88], PbO-PbF_2 [89], $Ba(Cu_{0.5}W_{0.5})O_3$, $BiFeO_3$ [90] and Li_2CO_3 [91]. The additives for lead-free ferroelectric materials are CuO [92], $K_{5.4}Cu_{1.3}Ta_{10}O_{29}$ [93], (Na,K)-germanate [94] and $BiFeO_3$ [95].

Glass frits are also used as additives for lowering the sintering temperature. The borosilicate glass phases [96], B_2O_3-Bi_2O_3-CdO [89, 97] or a mixture of boron oxide and silica [34, 98, 99, 100] have been added to lead-based ferroelectric thick films.

2.3 Processing of Ferroelectric Thick Films on Various Substrates

2.3.1.1 Ferroelectric Thick Films on Silicon

The piezoelectric thick-film structures deposited on silicon substrates have been intensively studied for various applications such as sensors, accelerometers and transducers. The advantage of using a silicon substrate is that it is a well-developed technology that offers the possibility of Si micromachining. It also enables the integration of the thick-film material and the electronics within a single chip.

To obtain a good functional response of the ferroelectric layer, lead-based materials require thermal treatment at a temperature between 800°C and 900°C. At these temperatures the volatility of the PbO and the interdiffusion of the lead oxide and Si through the bottom electrode are significant. As a result, SiO_2, which is commonly used as a passivation layer for a Si wafer, chemically reacts with the PbO and forms lead-silicate compounds at the substrate/electrode interface [101, 102]. Consequently, they lead to the delamination of the electrode from the silicon [103].

Various approaches have been used to improve the adhesion of the lead-based ferroelectric layer on the Si substrate. It was shown, for example, that the bottom electrode may act as a buffer layer. The interdiffusion of Si and PbO has not been observed through a continuous and dense gold electrode. Consequently, the delamination of the PZT from the Si substrate was avoided [104]. A PZT thick film with the addition of low-melting-point compounds was deposited on silicon, and a bilayer Au/Pt structure was used as an electrode. Good dielectric properties and a high d_{33} value of the thick-film structure were reported [97].

To improve the adhesion of the layer on the silicon substrate, and to minimise the chemical reactivity between the thick-film components, various structures have been reported. Si/SiO_2/Cr/Pt [54], Si/SiO_2/Ir/Pt [57, 63], Si/$SiO_2$$ZrO_2$/Pt [105], Si/$SiO_2$/YSZ/$TiO_2$/Pt [28, 29], Si/$SiO_2$/Ti/Pt [88], Si/$SiO_2$/$Si_3N_4$/$TiO_2$/Pt [103] and Si/$SiO_2$/$Al_2O_3$/Au [106] have been tested successfully.

2.3.1.2 Ferroelectric Thick Films on Ceramic Substrates

There are several potential applications of ferroelectric thick films on ceramic substrates, including gravimetric sensors [107] pyroelectric sensors [78, 83], ultrasound medical transducers [6, 85, 108, 109], microbalances [80], pressure sensors [36, 110] and electrophoretic printing [5, 30].

Alumina is a widely used material as a ceramic substrate because it is thermally stable and chemically inert. However, the presence of a small amount of oxides such as MgO, SiO_2, CaO in the alumina substrate causes the formation of secondary phases at the thick-film/substrate interface.

An example is a PLZT thick film on a platinised alumina substrate [111]. It was observed that during the processing the PLZT together with the bottom Pt electrode always peeled off the alumina substrate. The main reason was the formation of beta-alumina crystals at the interface between the alumina and the platinum.

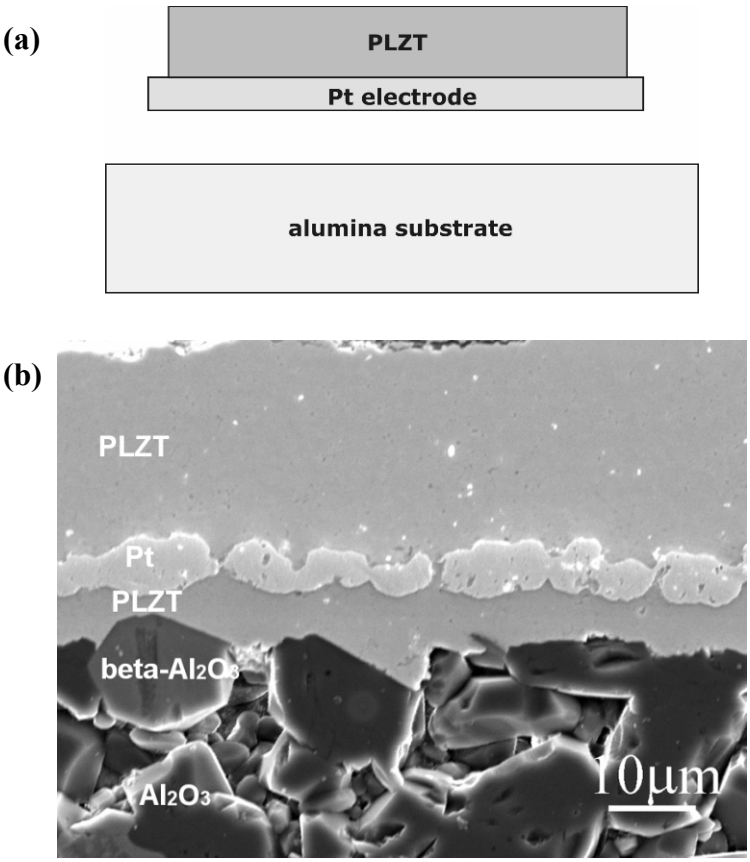

Fig. 2.4. a Schematic of the PLZT/Pt layer peeled of the alumina substrate; **b** PLZT barrier layer placed in between the alumina substrate and the Pt bottom electrode improves the adhesion between the PLZT layer and the substrate.

To avoid the delamination of active PLZT/Pt from the alumina substrate, the formation of undesirable large crystals at the Pt/alumina interface should be eliminated. The incorporation of an additional PLZT barrier layer between the alumina and the Pt electrode hinder the diffusion of Al_2O_3 into the active PLZT. It minimised the reaction products and, therefore, the undesirable reaction products are not formed at the alumina/Pt interface (Fig. 2.4) [5].

The weak adhesion between the bottom Pt electrode and the alumina substrate was applied for processing substrate-free PMN-PT bending-type actuators. Composites were peeled off from the substrates [112] after screen printing and firing the PMN-PT/Pt.

For some applications, such as micro-sensors or actuators, the ferroelectric thick-film structures tend to be integrated into low-temperature co-fired ceramic (LTCC). This is a key substrate material in micro-system technologies [104, 113]. LTCC exhibits a high chemically reactivity with ferroelectric materials at a typical temperature of 850^{o}C required for the processing. The considerable inter-diffusion of ions from the PZT to the LTCC and vice-versa modifies the chemical composition of the PZT layer. Consequently, a degradation of the PZT's functional response has been reported [114, 115].

PZT thick films on LTCC substrates with good functional responses have been reported by Gebhart *et al*. [104]. They used a dense, continuous gold bottom electrode that acts as a barrier layer.

Hrovat *et al.* [115] showed that an additional alumina layer imposed between the LTCC substrate and the bottom electrode also acts as a barrier. The functional response of a PZT thick film with a barrier layer is enhanced when compared to a barrier-free thick-film structure [116].

PZT-based ferroelectric thick-film structures have been studied for medical ultrasonic transducers. In order to integrate the PZT thick film and the backing, the thick PZT film was deposited on porous alumina or a porous PZT substrate [108, 117].

2.3.1.3 Ferroelectric Thick Films on Metals and Alloys

Metals and alloys have been used to replace silicon substrates due to their simple tooling and good robustness. However, any integration with ceramic ferroelectric thick-films is difficult.

PZT films have been processed on stainless steel using a modified sol-gel method [27], and the aerosol deposition technique [118, 119]. Good functional response of PZT films on stainless steel prepared at a temperature of around 600^{o}C has been reported. PZT thick-films have also been made on Ni substrates using screen printing. The excessive oxidation of Ni was partially suppressed by a double screen-printed Au electrode, with the first one being fired in argon [120]. The deposition of high-permittivity ferroelectric materials on copper is promising for embedded capacitor applications in printed circuit boards [46]. PZT has also

been deposited by electrophoretic deposition on copper foil. After sintering, a Cu_xPb alloy was formed, which deteriorated the properties of the PZT thick film.

A PZT ferroelectric thick film with an oxide bottom electrode has been demonstrated. A composite lead-ruthenate-PZT electrode was screen printed and fired on an alumina substrate, followed by screen-printed and sintered PZT [121].

2.4 Summary

A brief review of the processing features of ferroelectric thick films has been presented here. It is clear that the processing of ferroelectric thick films has advanced significantly in the past 15 years. This has been a typical application-driven research that has resulted in a number of practical solutions. More effort is needed in powder synthesis and in novel deposition methods. A better understanding of phenomena like constrained sintering, the physics and chemistry of interfaces, the general properties of thick films and, in particular, the processing-properties relationship is required.

2.5 Acknowledgment

The financial support of the Slovenian Research Agency and EU 6FP Network of Excellence MIND (NoE 515757-2) is gratefully acknowledged.

References

1. Dorey RA, Whatmore RW (2004) Electrical properties of PZT and PMN-PT/PZT thick films produced using ComFi technology. J. Eur. Ceram. Soc. 24:1091- 1094.
2. Kwon S, Sabolsky E, Messing GL (2001) Low-temperature re sintering of 0.65PMN-0.35PT. J. Am. Ceram. Soc. 84:648-650.
3. Dorey R A, Whatmore R W (2004) Electroceramic thick film fabrication for MEMS. J.Electroceram., 12:19-32
4. Guha JP, Hong DJ, Anderson, HU (1998) Effect of excess PbO on the sintering characteristic and dielectric properties of $Pb(Mg_{1/3}Nb_{2/3})O_3 – PbTiO_3$-based ceramics. J. Am. Ceram. Soc. 71:C152-154.
5. Kosec M, Holc J, Malič B, Bobnar V (1999) Processing of high performance lead lanthanum zirconate titanate thick films. J. Eur. Ceram. Soc. 19: 949-954.
6. Kosec M, Murko D , Holc J, Malič B, Čeh M, Hauke T, Beige H (2001a) Low-temperature processing of $(Pb,La)(Zr,Ti)O_3$ thick films on alumina substrates. Z. Met. Kd. 92: 97-104

7. Saha D , Sen A, Maiti H S (1999) Low temperature liquid phase sintering of lead magnesium niobate. Ceram. Int. 25:145-151
8. Bernik S, Marinenko RB, Holc J, Samardžija Z, Čeh M, Kosec M (2003) Compositional homogeneity of ferroelectrics (Pb,La)(Ti,Zr)O_3 thick films. J. Mat. Res. 18:515-523.
9. Kosec M, Holc J, Kuscer D, Drnovšek S (2007) Pb($Mg_{1/3}Nb_{2/3}$)O_3 – $PbTiO_3$ thick films from mechanochemically synthesized powder. J. Eur. Ceram. Soc. 27:3775-3778
10. Kuscer D, Kovač J, Tchernychova Šturm E, Kosec M (2009a) Characterisation of the amorphous phase and the nano-sized crystallites in high-energy-milled lead-magnesium-niobate powder, J. Am. Ceram. Soc. 92:1224-1229.
11. Kuscer D, Meden A, Holc J, Kosec M (2006) Mechano-Synthesis of Lead-Magnesium-Niobate Ceramics. J. Am. Ceram. Soc. 89:3081-3088
12. Kuscer D, Holc J, Kosec M (2007) Formation of Pb($Mg_{1/3}Nb_{2/3}$)O_3 -0.35 $PbTiO_3$ using a high-energy milling process. J. Am. Ceram. Soc. 90:29-35
13. Kuscer D, Skalar M, Holc J, Kosec M (2009) Processing and properties of 0.65 Pb($Mg_{1/3}Nb_{2/3}$)O_3 -0.35 $PbTiO_3$ thick films. J. Eur. Ceram. Soc. 29:105-113
14. Deng Y, Liu L, Cheng Y, Nan CW, Zhao S, (2003) Hydrothermal synthesis and characterisation of nanocrystalline PZT powders. Mat. Lett. 57:1675-78.
15. Chen X, Fan H, Ke S (2006) Low-temperature synthesis of (Pb,La)(Zr,Ti)O_3 thick-film on Ti substrates by the hydrothermal method using oxide precursors. Appl. Phys. Lett., 88:012901
16. Chen X, Fan H, Liu L, Ke S (2008) Low-temperature growth of lead-magnesium niobate thick films by hydrothermal process. Ceram. Int. 34:1063-66
17. Ndiaye PA, Loiseau B, Minaut S, Pernot P, Tricot JC (1999) $PbZr_xTi_{1-x}O_3$ hydrothermal synthesis on titanium substrate for actuators. Myrosystem Techn. 6:15-18.
18. Ndiaye PA, Loiseau B, Minaut S, Pernot P, Tricot JC (1999) $PbZr_xTi_{1-x}O_3$ hydrothermal synthesis on titanium substrate for actuators. Myrosystem Techn. 6:15-18.
19. Heinrich JG, Kim JW (2005) Influence of processing parameters on microstructure and ferroelectric properties of PZT-coated SiC fibers J. Eur. Ceram. Soc. 25:1637-45
20. Rodrigues JB and Eiras JA (2002) Preparation and characterization of PLT thick-films produced by a chemical route J. Eur. Ceram. Soc. 22:2927-2932
21. Simon L, Le Dren S, Gonnard P (2001) PZT and PT screen-printed thick films. J. Eur.Ceram.Soc 21:1441-1444
22. Lee DY, Yu JH, Shin YS, Park D, Yu TU, Hwang J (2008) Formation of ceramic nano-particle patterns using electrohydrodinamic jet printing with pin –to-pin electrodes. J. Appl. Phys. 47:1723-25
23. Prudenziati M (1994) Thick Film Sensors, Handbook of Sensors and Actuators 1, Elsevier, Amsterdam
24. Harper C A (1974) Handbook of Thick Film Hybrid Microelectronics, McGraw-Hill, New York
25. Torah RN, Beeby SP, Tudor MJ, White NM (2007) Thick film piezo ceramics and devices. J. Electroceram. 19:95-110.
26. Lucat C, Menil F, Von Der Mühll R. (1997) Thick-film densification for pyroelectric sensors. Meas. Sci. Technol. 8:38-41.
27. Zhou Q F, Chan H L W, Choy C L, (2000) PZT ceramic/ceramic 0–3 nanocomposite films for ultrasonic transducer applications. Thin Solid Films, 375:95-99
28. Kim Y B, Kim T S, Choi K S, Choi D J (2001) Densification method of screen printed PZT(52/48) thick films. Integrated Ferroelectrics 35:199-208
29. Kim YB, Kang JY, Kim TS (2002), Fabrication and Resonant Behavior of PZT Thick Film Cantilever for BioChip. Integrated Ferroelectrics 50:11-20
30. Gebhardt S, Seffner L, Schönecker A, Rödel J, Beckert W, Kreher W, Sotnikov A, Häßler W, Reuter S, Hübler A (2004) Bi-layered PZT films by combining thick and thin film technology. J. Eur. Ceram. Soc. 24:1101-1105

31. Wang Z, Zhu W, Zhao C, Tan O K (2003) dense PZT thick films derived from sol-gel based nanocomposite process. Materials Science and Engineering B 99:56-62
32. Corker D L, Zhang Q, Whatmore R W, Perrin C (2002) PZT composite ferroelectric thick films, J. Eur. Ceram. Soc. 22:383-390
33. Dorey RA, Stringfellow S B, Whatmore R W, (2002) Effect of sintering aid and repeated sol infiltration on the dielecrric and piezoelectric properties of PZT composite of a PZT composite thick film. J. Eur. Ceram. Soc., 22:2921-2926
34. Koch M, Harris N, Evans AGR, White NM, Brunnschweiler A, (1998) A novel micromachined pump based on thick-film piezoelectric actuation. Sensors and Actuators A 70:98-103
35. Reed J S (1995) Principles of Ceramics Processing, Second Addition, John Wiley & Sons, Inc. New York
36. Belavič D, Hrovat M, Holc J, Santo-Zarnik M, Kosec M, Pavlin M (2008) The application of thick-film technology in C-MEMS. J. Electroceram. 19:363-368.
37. Golonka LJ (2003) Low temperature cofired ceramics (LTCC) technology in microelectronics. In: Kosec M, Malič B, Kuščer D (eds) Conference Notes, Processing of Electroceramics, Bled, August 31-September 3, 2003, pp 313-329.
38. Wolny WW (2000) Proc. 12th IEEE Int. Symp. on Applications of Ferroelectrics, ISAF 2000, Honolulu, July 21-August 2, pp 257-262.
39. Zhitomirsky I (2002) Cathode electro deposition of ceramic and organoceramic materials. Fundamental aspects. Advances in Colloid and Interface Science 97:279-317
40. Tabellion J, Clasen R (2004) Electrophoretic deposition from aqueous suspension for near shape manufacturing of advanced ceramics and glasses-applications. Journal of Material Science 39:803-811.
41. Sarkar P, Nicholson P S (1996) Electrophoretic deposition (EPD): mechanisms, kinetics, and application to ceramics. J. Am. Ceram. Soc. 79:987-2002
42. Kaya C, Kaya F, Su B, Thomas B, Boccaccini AR (2005) Structural and functional thick ceramic coatings by electrophoretic deposition. Surface and Coatings Techn. 191:303-310
43. Su B., Ponton CB, Button TW (2001) Hydrothermal and electrophoretic deposition of lead zirconate titanate (PZT) films. J. Eur. Ceram. Soc., 21:1539-42
44. Ng SY, Boccaccini AR (2005) Lead zirconate titanate films on metallic substrates by electrophoretic deposition. Mater. Sci. Eng. B 116:208-214
45. Van Tassel J, Randall CA (1999) Electrophoretic deposition and sintering of thin/thick PZT films. J. Eur. Ceram. Soc. 19:955-958
46. Wu A, Vilarinho PM, Kingon AI (2006) Electrophoretic deposition of lead zirconate titanate films on metal foils for embedded components. J. Am. Ceram. Soc. 89:575-581
47. Wu A, Vilarinho PM, Srinivasan S, Kingon AI, Reanay IM, Woodward D, Ramos AR, Alvis E (2006a) Microstructural studies of PZT thick films on Cu foils. Acta Materialia 54:3211-3220
48. Windle J, Derby B (1999) Ink-jet printing of PZT aqueous ceramic suspensions, J. Mater. Sci. Lett. 18:87-89.
49. Senslis G, Dubarry M, Lejeune M, Chartier T (2002) 3D piezoelectric structure made by ink-jet printing. Ferroelectrics 273:279-284
50. Wang T, Derby B (2005) Ink-jet printing and sintering of PZT. J. Am. Ceram. Soc. 88:2053-58
51. Bhati AB, Mott M, Evans JRG, Edirishinge MJ (2001) PZT pillars for 1-3 composited prepered by ink-jet printing, J. Mater. Sci. Lett. 20:245-48
52. Lejeune M, Cartier T, Dossou-Yovo C, Noguera R (2009) Ink-jet printing of ceramic micro-pillar arrays. J. Eur. Ceram. Soc. 29:905-911
53. Noguera R, Lejeune M, Cartier T (2005) 3D fine scale ceramic components formed by ink-jet prototyping process. J. Eur. Ceram. Soc. 25:2055-59

54. Adachi H, Kuroda Y, Imahashi T, Yanagisawa K (1997) Preparation of Piezoelectric Thick Films using a Jet Printing System. Jpn. J. Appl. Phys. 36:1159- 1163
55. Akedo J, Lebedev M, Sato H, Park J (2005) High-speed optical microscanner driven with resonation of lam waves using $Pb(Zr,Ti)O_3$ thick films formed by aerosol deposition. Jap. J. Appl. Phys. 44:7072-7
56. Choi JJ, Hahn BB, Ryu J, Yoon WH, Park DS (2007) Effect of PZN addition and post annealing temperature on electrical properties of PZT thick films prepared by aerosol deposition method. J. Appl. Phys. 102:044101
57. Lebedev M, Akedo J, Akiyama Y (2000) Actuation Properties of Lead Zirconate Titanate Thick Films Structured on Si Membrane by the Aerosol Deposition Method. Jpn. J. Appl. Phys. 39:5600-5603
58. Stytsenko E, Ryan MJ, Daglish M (2004) Airflow deposition of oxide electroceramic films. J. Eur. Ceram. Soc. 24:999-1003
59. Schubring N W, Mantese J V, Micheli A L, Catalan A B, Mohammed M S, Naik R, Auner G (1999) Graded ferroelectrics: a new class of steady state thermal/electrical/mechanical elergy interchange devices. Integrated Ferroelectrics 24:155-168
60. Ledermann N, Muralt P, Gentil S, Mukati K, Cantoni M, Baborowski J, Settter N, (2003) {1 0 0}-Textured, piezoelectric $Pb(Zr_xTi_{1-x})O_3$ thin films for MEMS: integration, deposition and properties. Sensors and Actuators A 105:162-170
61. Takashi I, Imai S, Matsuda H, (2004) fabriaction of lead zirconate titanate thick film discs for micro transducers devices. Mat. Res. Soc. Proc. 785: D4.5.1-D4.5.6.
62. He XY, Ding AL, Zheng XS, Qiu PS, Luo WG (2003) Preparation of PZT(53/47) thick films deposited by a dip-coating process. Microelectronic Engineering, 66:865-871
63. Tsurumi T, Ozawa S, Abe G, Ohashi N, Wada S, Yamane M, (2000) Preparation of PZT(53/47) thick films deposited by a dip-coating process. Jpn. J. Appl. Phys. 39:5604-5608
64. King B H, Dimos D, Yang P, Morissette S L (1999) Direct-write fabrication of integrated, multilayer ceramic components. Journal of Electroceramics 3:173-78
65. Morissette S L, Lewis J A, Clem P G, Cesarano J, Dimos D B (2001) Direct-Write Fabrication of $Pb(Nb,Zr,Ti)O_3$ Devices: Influence of paste rheology on print morphology and component properties. J. Am. Ceram. Soc. 84: 2462-2468
66. Sarkar-Deliormanh A, Celik E, Polat M (2008) Rheological behavior of PMN gels for solid freeform fabrication. Colloids and Surfaces A: Physicochemical and Engineering Aspects 324:159-66
67. Smay J E, Cesarano III J, Tuttle B A, Lewis J A, (2004) Directed Colloidal Assembly of Linear and Annular Lead Zirconate Titanate Arrays. J. Am. Ceram. Soc. 87:293-295
68. Guo D, Cai K, Li L, Zhilun Gui Z, (2003) Application of gelcasting to the fabrication of piezoelectric ceramic parts. J. Eur. Ceram. Soc. 23:1131-37
69. Guo D, Li L, Cai K, Gui Z, Nan C (2004) Rapid Prototyping of Piezoelectric Ceramics via Selective Laser Sintering and Gelcasting. J. Am. Ceram. Soc. 87:17-22
70. Sun D, Rocks SA, Wang D, Edirisinghe MJ, Dorey RA (2008) Novel forming of columnar lead zirconate titanate structures. J. Eur. Ceram. Soc. 28:3131-39
71. Bordia R K, Raj R, (1985) Sintering behaviour of ceramic films constrained by a rigid substrate. J. Am. Ceram. Soc. 68:287-292.
72. Mohanram A, Lee S, Messing GL, Green DJ (2006) Constrained sintering of Low-Temperature Co-Fired Ceramics. J. Am. Ceram. Soc. 89: 1923-1929
73. Tzeng SY, Jean JH (2002) Stress development during constrained sintering of alumina/glass/alumina sandwich structure J. Am. Ceram. Soc. 85:335-340
74. Härdtl KH, Rau H (1969) PbO vapour pressure in the $Pb(Ti_{1-x})O_3$ system. Solid State Commun. 7:41-45

75. Kosec M, Holc J, Levassort F, Tran-Huu-Hue P, Lethiecq M (2001) Screen-printed $Pb(Zr,Ti)O_3$ thick films for ultrasonic medical imaging applications. International Symposium on Microelectronics, Baltimore, Maryland. Proceedings. Washington: IMAPS, pp 195-200
76. Kuscer D, Korzekwa J, Kosec M, Skulski R (2007a) A- and B-compensated PLZT x/90/10: Sintering and microstructural analysis. J. Eur. Ceram. Soc. 27 :4499-4507
77. Fushimi S, Ikeda T (1967) Phase Equilibrium in the System $PbO-TiO_2–ZrO_2$. J. Am. Ceram. Soc., 50:129-132
78. De Cicco G, Morten B, Dalmonego D, Prudenziati M (1999) Pyroelectricity of PZT-based thick-films. Sensors and Actuators A, 76:409-415.
79. Ferrari V, Marioli D, Taroni A (1997) Thick-film resonant piezo-layers as new gravimetric sensors. Meas. Sci. Technol. 8:42-48.
80. Ferrari V, Marioli D, Taroni A, Ranucci E (2000) Multisensor array of mass microbalances for chemical detection based on resonant piezo-layers of screen-printed PZT. Sensors and Actuators, B 68:81-87
81. Futakuchi T, Nakano K, Adachi M (2000) Low-Temperature Preparation of Lead-Based Ferroelectric Thick Films by Screen-Printing. Jpn. J. Appl. Phys. 39:5548-5551
82. Lee BY, Cheon CI, Kim JS, Bang KS, Kim JC, Lee HG (2002) Low temperature firing of PZT thick films prepared by screen printing method. Materials Letters 56:518-521
83. Lozinski A, Wang F, Uusimäki A, Leppävuori, (1997) PLZT thick films for pyroelectric sensors. Meas. Sci. Technol. 8:33-37
84. Belavič D, Santo Zarnik M, Holc J, Hrovat M, Kosec M, Drnovšek S, Cilenšek J, Maček S (2006) Properties of Lead Zirconate Titanate Thick-Film Piezoelectric Actuators on Ceramic Substrates. Int. J. Appl. Ceram. Techn. 3: 448-454
85. Tran-Huu-Hue P, Levassort F, Meulen FV, Holc J, Kosec M, Lethiecq M (2001) Preparation and electromechanical properties of PZT/PGO thick films on alumina substrate. J. Eur. Ceram. Soc. 21:1445-1449
86. Akiyama Y, Yamanaka K, Fujisawa E, Kowata Y (1999) Development of lead zirconate titanate family thick films on various substrates. Jpn. J. Appl. Phys. 38:5524-5527
87. Chen HD, Udayakumar KR, Cross LE, Bernstein JJ, Niles LC (1995) Dielectric, ferroelectric, and piezoelectric properties of lead zirconate titanate thick films on silicon substrates. J. Appl. Phys. 77:3349-3353
88. Simon-Seveyrat L, Gonnard P (2003) Processing and characterization of piezoelectric thick films screen-printed on silicon and glass-ceramic substrates. Integrated Ferroelectrics 51:1-18
89. Le Dren S, Simon L. Gonnard P, Troccaz M, Nicolas A (2000) Investigation of factoers affecting the preparation of PZT thick films. Mat. Res.Bull. 35:2037-45.
90. Kaneko S, Dong D, Murakami K (1998) Effect of Simultaneous Addition of $BiFeO_3$ and $Ba(Cu_{0.5}W_{0.5})O_3$ on Lowering of Sintering Temperature of $Pb(Zr,Ti)O_3$ Ceramics. J. Am. Ceram. Soc. 81: 1013-1018
91. Gentil S, Damjanovic D, Setter N (2005) Develpoment of relaxor ferroelectric materials for screen-printing on alumina and silicon substrates. J. Eur. Ceram. Soc. 25:2125-2128
92. Matsubara M, Toshiaki Y, Sakamoto W, Kikuta K, Yogo T, Hirano S (2005) processing and piezoelectric propeorties of lead-free $(K,Na)(Nb,Ta)O_3$ ceramics. J. Am. Ceram. Soc. 88:1190-96
93. Matsubara M, Yamaguchi Y, Kikuta K, Hirano S (2005a) Sintering and piezoelectric properties of potasium niobate ceramics with newly developed syntering aid. Jpn. J. Appl. Phys. 44:258-63.
94. Bernard J, Benčan A, Rojac T, Holc J, Malič B, Kosec M (2008) Low-temperature sintering of $K_{0.5}Na_{0.5}NbO_3$ ceramics. J. Am. Ceram. Soc. 91:2409-2411.
95. Zuo R, Ye C, Fang X (2008) $Na_{0.5}K_{0.5}NbO_3$-$BiFeO_3$ lead-free piezoelectric ceramics. J. Phys. Chem. Solids, 69:230-235

96. Thiele ES, Setter N (2000) Lead zirconate titanate particle dispersion in thick film ink formulation. J. Am. Ceram. Soc. 83:1407-12.
97. Thiele ES, Damjanović D, Setter N J. (2001) Processing and Properties of Screen-Printed Lead Zirconate Titanate Piezoelectric Thick Films on Electroded Silicon. J. Am. Ceram. Soc. 84:2863-2868
98. Beeby SP, Blacburn A, White NM (1999) Processing of PZT piezoelectric thick films on silicon for microelectromechanical systems. J. Michromech. Microeng. 9:218-229
99. Jones GJ, Beeby SP, Dargie P, Papakostas T, White N (2000) An investigation into the effect of modified firing profiles on the piezoelectric properties of thick-film PZT layers on silicon Measurement Science and Technology 11:526-531
100. Koch M, Harris N, Maas R, Evans AGR, White NM, Brunnschweiler A, (1997) A novel micropump design with thick-film piezoelectric actuation. Meas. Sci. Technol. 8:49-57.
101. Glynne -Jones P, Beeby SP, Dargie P, Papakostas T, White NM (2000) An investigation into the effect of modified firing profiles on the piezoelectric properties of thick-film PZT layers on silicon. Meas. Sci. Technol. 11:526-531.
102. Smart RM, Glasser FP (1974) Compound Formation and Phase Equilibria in the System PbO-SiO_2. J. Am. Ceram. Soc. 57:378-382.
103. Duval FCC, Dorey RA, Haigh RH, Whatmore RW (2003) Stable TiO_2/Pt electrode structure for lead containing ferroelectric thick films on silicon MEMS structures. Thin Solid Films, 444:235-240.
104. Gebhardt S, Seffner L, Schlenkrich F, Schonecker A (2007) PZT thick films for sensor and actuator applications. J. Eur. Ceram. Soc. 27:4177-80.
105. Jeon Y, Kim DG, No K, Kim S J, Chung J (2000) Residual stress analysis of Pt bottom electrodes on ZrO_2/SiO_2/Si and SiO_2/Si substrates for Pb(ZrTi)O_3 thick films. Jap. J. Appl. Phys. 39:2705-2709
106. Kosec M, Holc J, Hauke T, Beige H (2001b) PZT based thick films on silicon. Abstracts of the 10th International Meeting on Ferroelectricity, IMF 10, Madrid, (Spain)
107. Huang Z, Zhang Q, Corkovic S, Dorey R A, Duval F, Leighton G, Wright R, Kirby P, Whatmore R W (2006) Piezoelectric PZT films for MEMS and their characterisation by interferometry. J. Electroceram. 17:549-556
108. Maréchal P, Haumesser L, Tran-Huu-Hue LP, Holc J, Kuscer D, Lethiecq M, Feuillard G (2008) Modeling of a high frequency ultrasonic transducer using periodic structures. Ultrasonics 2:141-149.
109. Maréchal P, Levassort F , Holc J, Tran-Huu-Hue LP, Kosec M, Lethiecq M (2006) High-frequency transducers based on integrated piezoelectric thick films for medical imaging. IEEE Trans. Ultrason. Ferroelectr. Freq. Control 53:1524-1533.
110. Santo Zarnik M, Belavič D, Maček S, Holc J (2009) Feasibility study of a thick-film PZT resonant pressure sensor made on a prefired 3D LTCC structure. Int. J. Appl. Ceram. Techn. 6:9-17.
111. Holc J, Hrovat M, Kosec M (1999) Interactions between alumina and PLZT thick films. Mat.Res.Bul., 34:2271-78.
112. Uršič H, Hrovat M, Holc J, Santo-Zarnik M, Drnovšek S, Maček S, Kosec M (2008b) A large-displacement 65Pb($Mg_{1/3}Nb_{2/3}O_3$-35$PbTiO_3$/Pt bimorph actuator prepared by screen printing. Sensors and Actuators B 133:699-704.
113. Golonka LJ, Buczek M, Hrovat M, Belavic D, Dziedzic A, Roguszczak H, Zawada T (2005) Properties of PZT thick films made on LTCC. Microelectronics International 22:13-16
114. Hrovat M. Holc J, Drnovšek S, Belavic D, Bernard J, Kosec M, Golonka L, Dziedzic A, Kita J (2003) Characterization of PZT thick films fired on LTCC substrates. J. Mat. Sci. Lett. 22:1193-1195.
115. Hrovat M, Holc J, Drnovšek S, Belavič D, Cilenšek J, Kosec M (2006) PZT thick films on LTCC substrate with imposed alumina barrier layer. J. Eur. Ceram. Soc. 26:897-900.

116. Uršič H, Hrovat M, Belavič D, Cilenšek J, Drnovšek S, Holc J, Santo-Zarnik M, Kosec M (2008a) Microstructural and electrical characterisation of PZT thick films on LTCC substrates. J. Eur. Ceram. Soc. 28:1839-44.
117. Levassort F, Holc J, Ringaard E, Bove T, Kosec M, Lethiecq M (2007) Fabrication, modelling and use of porous ceramics for ultrasonic transducer applications. J. Electroceram. 19:125-137.
118. Akedo J, Lebedev M (2000) Piezoelectric properties and poling effect of $Pb(Zr,Ti)O_3$ thick films prepared for microactuators by aerosol deposition. Appl. Phys. Lett. 77:1710-1712.
119. Park JH, Akedo J, Sato H. (2007) High-speed metal-based optical microscanners using stainless-steel substrate and piezoelectric thick films prepared by aerosol deposition method Sensors and Actuators A 135:86-91
120. Benčan A, Holc J, Hrovat M, Dražić G, Kosec M (2002) Interactions between PZT thick films and Ni substrates. Key Eng. Mater. 206-213:1301-1304.
121. Holc J, Hrovat M, Kuščer D, Kosec M (2002) The preparation and properties of a PZT thick film on an alumina substrate with a $Pb_2Ru_2O_{6.5}$ electrode. Ferroelectrics, 270:87-92.

Chapter 3
Tailored Liquid Alkoxides for the Chemical Solution Processing of Pb-Free Ferroelectric Thin Films

Kazumi Kato

3.1 Tailored Alkoxides

The chemical solution deposition method has been applied widely for multicomponent thin films. Generally, its high potential is attributable to the homogeneity of solutions. However, low affinity among conventional raw materials such as metalorganic compounds and organic solvents sometimes remains problematic. Tailoring the molecular structure of a liquid source and optimising its solubility and reactivity for hydrolysis, condensation, and combustion would yield the following: a precisely controlled composition, low-temperature crystallisation, high phase purity, and uniform microstructure in a thin film deposited using a liquid source [1, 2, 3]. In particular, low-temperature crystallisation is essential for integration of ferroelectric thin films into semiconductors.

3.2 $Sr[BiTa(OR)_9]_2$ and $Sr[BiNb(OR)_9]_2$ for $SrBi_2Ta_2O_9$ and $SrBi_2Nb_2O_9$

3.2.1 Chemistry in Solutions of Sr-Bi-Ta and Sr-Bi-Nb Complex Alkoxides [*3*, *4*]

Precursors for thin films of layer-structured perovskite $SrBi_2Ta_2O_9$ and $SrBi_2Nb_2O_9$ were prepared by the reactions of a strontium-bismuth double methoxyethoxide and tantalum or niobium methoxyethoxide in methoxyethanol,

National Institute of Advanced Industrial Science and Technology (AIST), 2266-98 Anagahora, Shimoshidami, Moriyama-ku, Nagoya 463-8560, Japan